ARTICLE | Article in Press

An integrated machining performance framework considering tool wear and hole integrity attributes during drilling via indexable drilling inserts using entropy-weights and TOPSIS

Muhammad Farzik Ijaz · Muhammad Zubair Afzal · Samina Ishtiaq · Sarmad Ali Khan · Muhammad Umar Farooq · Saqib Anwar

Received: 27 June 2026 / Accepted: 27 October 2026
© The Author(s) 2026

Abstract

Quantification of machinability is challenging, especially with the development of new materials like DC 53 steel and new tooling, such as the fabrication of indexable inserts. In this context, an integrated machining performance framework named the Integrated Hole Integrity Index (IHII) is proposed. An indexable drilling setup with peripheral wiper inserts and central stepped carbide inserts was employed. The drilling tests were conducted at 20 m/min and 30 m/min cutting speeds while employing feed rates of 0.05 mm/rev, 0.075 mm/rev, and 0.10 mm/rev to assess the effect of microstructure on tool wear, surface integrity, diametric error, machining temperature, and burr formation. The microstructural examination revealed that D2 steel contained large carbides that were not evenly distributed, but DC53 steel displayed a martensitic structure with small carbides that were evenly spaced. The D2 steel performed better than DC53 steel such that the minimum flank wear value of 49 µm was recorded when drilling the former material at 20 m/min and 0.05 mm/rev, with surface roughness values being in the range of 1.0–4.8 µm. However, tool wear was almost in the same vicinity, but roughness values were substantially higher, ranging from 1.9 to 5.4 µm with the latter material at the same machining parameters. The SEM analysis revealed that surface damage occurred through three main mechanisms, which included adhesion, material side flow, and plastic deformation. For a more holistic drilling performance assessment, an IHII model/performance metric is calculated using entropy weights and subsequently TOPSIS analysis was conducted to overcome the limitations of individual output responses. Hereafter, the best drilling condition is suggested, which indicates the best compromise among all output responses. A value of 0.743 for IHII was calculated for Test 4, performed on D2 material, showing a better performance index, while a 23% lower IHII was determined for DC53 steel.

Keywords D2 steel · DC 53 steel · Microstructure · Drilling · Integrtared hole integrity index

This Article in Press is shared early to give you faster access to new research. It is citable and carries a permanent DOI. The final edited version will replace it automatically.

https://doi.org/10.1038/s41598-026-78568-1

Published online: 15 November 2026

scientific reports

Introduction

The manufacturing collaborative working group recently highlighted the need for integrated machining performance, with a special focus on uncovering the machining potential of cutting tools. Standardization and quantification of machinability were identified as the major challenge. A data-driven approach and a need for a more holistic machining assessment were established[1]. In this study, various methods were proposed to enhance machinability, and engineering tool design was identified as one possible solution in this context. Tools with novel designs provide substantial competition to generic tool geometries. Over the years, various tool edge geometries were evaluated for specific combinations and, to the best of the authors' knowledge, this aspect is proven to be tool-workpiece and condition-specific. Tool texturing is another emerging area with various types of textures imparted on cutting tools, and some productivity gains were reported[2]. Wiper configuration on turning inserts has now been well established[3], but their use in drilling is restricted. In drilling, a major breakthrough at macro-level geometry was achieved with Indexable inserts. These inserts provide not only cost benefits with the provision of indexing and replacement benefits, as opposed to the need to replace the whole solid drill bits. These inserts provide the synergistic benefits of central step technology with a wiper peripheral insert. Additionally, the provision of various chip breaker designs with a groove width and depth can significantly enhance the machinability aspect with better chip breakability. The current work is an attempt to explore this novel Indexable drilling technology on relatively new DC 53 and conventional D2 steels, where the former has now been considered as a potential alternative to the latter material. For holistic drilling performance considering various machining attributes including tool wear, surface roughness, diametric error, machining temperature, and exit burr height, an integrated hole integrity index performance metric is proposed. In view of the building context, a literature review is presented, and at the end of this section, the need for the current work is established.

Steels have long been the foremost engineering material, extensively used in production sectors, with ongoing and extensive research into their machinability[4]. Among all steels, D-series tool steels are high-carbon, chromium cold work steels widely used in die and mold applications owing to their high wear resistance and higher hardness. Among the D-series, D2 steel is most commonly used owing to its balanced combination of hardness and wear resistance. Recently, modified grades such as DC53 steel have been developed to enhance toughness through refined microstructural control alongside similar wear performance[5]. Although DC53 steel has less carbon and chromium (1% and 8%, respectively) than D2, the inclusion of Mo, V, and W contributes to its high hardness[6,7]. Controlling the cooling rates and solidification leads to improved toughness through primary carbide refining and homogeneous distribution; thus, this material has the potential to substitute D2 steel in the die and mold industry[8]. Therefore, the process of machining these steels becomes difficult because these materials possess high toughness and better hardness, specifically in drilling, where the cutting zone is located deep inside the workpiece. These traits make drilling more difficult, resulting in rapid tool wear, higher drilling resistance, and higher machining temperatures. The materials also show high ductility, which results in chip clogging during drilling operation. The latter factor contributes to poor heat evacuation from the cutting zone, which can lead to surface damage and poor hole quality. Furthermore, heat generation also affects surface quality by creating microstructural changes and surface stresses that remain after machining[9]. A recent review comprehensively summarized the application of smart manufacturing systems in drilling and hole machining processes, highlighting the use of sensors such as vibration, cutting force, temperature, current, and acoustic signals for tool condition monitoring. The study emphasized that sensor-based monitoring can significantly improve tool wear prediction, surface integrity, dimensional accuracy, and chip morphology, thereby enhancing the overall machining performance[10].

Many studies found in the literature that focused on dry machining have been done with conventional solid carbide drills or high-speed steel (HSS) drill bits. The first study was on dry machining and focused on reducing the environmental footprint. The authors point out that the inclusion of surface textures or patterns on cutting tools can work towards machinability improvement when cutting in dry mode. In addition, the work also identifies how tool coatings contribute to+ saving costs by increasing the tool life[11]. Another study presents the chip

generation mechanism in relation to the cutting performance under dry machining conditions by hybrid textured cutting (HTT) inserts. The results show that such tools reduce cutting force as well as interface temperature, surface roughness, and tool wear in comparison with untextured tools. The investigation reveals that the use of dry HTT will lead to a better manufacturing process with an overall higher quality of finished products[12]. Minimum Quantity Lubrication (MQL) is typically thought of as a green alternative for dry processes. MQL is able to have a critical impact on the tool life and surface quality by decreasing cutting zone temperature and cutting force. This method may substitute for dry and wet lubrication successfully to achieve better performance in machining[13]. A recent study on the sustainable turning of Nitronic-50 using uncoated carbide inserts reported that sustainable quantity lubrication (SQL) significantly outperformed dry machining. Among the tested eco-friendly lubricants, propylene glycol–water and soap water provided the best performance, reducing cutting force, tool-tip temperature, friction, flank wear, and improving surface integrity, thereby demonstrating the effectiveness of green SQL strategies for sustainable machining[14]. Likewise, another study investigated the sustainable machining of Nitronic-50 using multilayer MT-CVD and MT-PVD coated inserts under small quantity lubrication (SQL). The results demonstrated that SQL, particularly with soap water and propylene glycol–water, significantly reduced cutting forces, tool-tip temperature, flank wear, and surface roughness while improving chip morphology and residual stresses[15]. Along similar lines, a recent study investigated the drilling of Al6082 alloy under dry, flood, MQL, and minimum quantity solid lubrication (MQSL) conditions. The results demonstrated that MQSL with MoS_2 nanoparticles significantly improved hole surface quality, reduced tool wear, and enhanced chip evacuation compared with conventional lubrication techniques, highlighting the potential of sustainable lubrication strategies for improving drilling performance[16]. Similarly, the sustainable turning of AISI 4140 steel under dry and MQL conditions showed that MQL reduced energy consumption by 42%, while machine learning models accurately predicted cutting force, cutting temperature, and surface roughness, demonstrating the potential of intelligent and sustainable machining[17]. Bio-based alternatives combined with MQL are also recommended by a few authors for achieving sustainability in machining, as traditional cutting fluids contribute to environmental harm[18]. The current technological development work focuses on enhancing dry machining operations through the development of advanced systems that provide better performance and easier operation. This includes creating more durable ceramic tools and developing energy-efficient methods for dry cutting[19]. The existing research suggests that, even though dry machining has some environmental benefits, further study and technological advancements are needed to improve its use in industry, particularly in drilling operations with materials like D2 steel.

For DC 53 steel, limited literature is available on the machining, focusing mainly on turning and milling only. The research studied DC53 steel machinability performance through turning operations by evaluating modified inserts (a combination of square and rhomboid design) with various hardness levels and different cutting parameter configurations. The research results showed that workpiece hardness proved to be the leading factor that influenced all measured parameters, including tool life, material removal, surface roughness, and cutting temperature. The SEM analysis showed that the coating failed through delamination, but the main failure causes included both surface adhesion loss and three types of wear, which depended on material hardness. The research established that DC53 steel can be used for productive turning operations because it achieves a minimum surface roughness (Ra) of 0.90 µm when using feed rates below 0.20 mm/rev[5]. Similarly, another study investigated how dry turning DC53 steel with Xcel carbide inserts affects tool longevity and surface finish quality based on different cutting speed, feed rate, and depth of cut settings. The study revealed that operating at 100 m/min cutting speed produced the optimal results because it extended tool lifespan to 39 min while producing the lowest surface roughness at 0.20 µm-Ra. At higher feed rates, material removal was maximized with acceptable surface quality, though at the cost of higher power consumption. The SEM and EDX analyses revealed that the material surface became attached to other materials, while its surface experienced wear from attrition and developed work hardening, which extended to 900 µm deep. The research recommended the use of Xcel inserts for environmentally friendly steel DC53 machining operations at higher feed rates[9]. Besides drilling, surface integrity has also been extensively investigated in other machining processes. Previous studies have examined the influence of grinding parameters on the surface integrity of D2 steel, whereas hole-making through helical milling has been used to

evaluate the effects of machining parameters and cooling strategies on surface quality and tool wear. These studies collectively demonstrate that surface integrity is a key indicator of machining performance regardless of the hole-making process employed, thereby reinforcing the need for comprehensive hole quality assessment in the present study[20–22].

Previous research studies have demonstrated that machining efficiency can be improved via tool texturing and use of various cutting environments such as MQL and MQSL. Bio-based cutting fluids have also increased over the years and shown substantial improvements. Specifically, conventional machinability of DC 53 steel has been exclusively focused on the turning process, with no reports on the drilling aspect. While D2 steel was drilled conventionally with solid carbide drills and milling cutters via the helical milling technique. On another side, Indexable inserts have proved their efficiency in difficult-to-machine materials such as superalloys[23] and composites[24], while this combination has not been evaluated on steels so far. In one of the initial studies, the combination of central stepped inserts with peripheral wiper inserts has emerged as a new solution that demonstrates better results than solid carbide drills in the drilling process when drilling Inconel 718[23]. Similarly, a recent comparative study evaluated the drilling performance of indexable and solid carbide drills while machining GFRP–steel hybrid composites. The results demonstrated that indexable drills exhibited lower tool wear, superior surface finish, improved dimensional accuracy, and lower drilling temperatures. These improvements were primarily attributed to their optimized cutting-edge geometry, efficient chip evacuation, and reduced thermal loading, highlighting the potential of indexable drills for machining difficult-to-cut materials[24]. The ongoing difficulties in drilling these steel materials, mainly due to their unique carbide structure, the properties of the matrix, and the limitations of current drilling tools, highlight the need for new tool design. Building on this idea, the current study examines the drilling performance of D2 and DC53 steels using an innovative tool configuration that combines central stepped carbide inserts and peripheral wiper inserts with LM chip-breaker geometry having a TiAlN PVD coating. The tool contains central inserts that employ stepped cutting edges for better chip breakability and reduce contact length. The other insert was a peripheral wiper insert that uses wiper-edge technology to improve surface quality due to its much straighter edge, which contributes to reducing the machined surface cusp heights. The research establishes direct connections between the D2 steel microstructure containing large irregular carbides and the DC53 steel microstructure with its fine carbide distribution in the matrix and their corresponding drilling results. Drilling results were evaluated in terms of tool wear, chip analysis, surface integrity, machining temperature, diametric error, and burr height (both quantitative and qualitative). Based on entropy weights of all output responses, the Integrated hole integrity index (IHII) is calculated, and all tests are ranked accordingly. At the end, tests were recommended for both D2 and DC 53 steels.

Experimental work

In the present study, the drilling experiments were conducted on the DC53 and D2 steel plates as workpiece materials under controlled cutting conditions. The chemical compositions of the workpiece materials were measured using an optical emission spectrometer, while their hardness values were determined by using the Rockwell C hardness test. Table 1 presents the chemical compositions of the selected workpiece materials along with their corresponding specifications and hardness values, respectively. In order to distinguish the influence of prior microstructural features on the corresponding hardness values and resulting machining characteristics of both workpieces, the systematic optical microstructural characterization of both workpieces was also performed. Figures 1(a) and (b) display the microstructure of DC53 steel, which predominantly consists of a martensitic matrix containing cementite along with finely dispersed primary and secondary carbide phases that are distributed randomly throughout the entire microstructure. It is noteworthy that the carbide distribution in the matrix is highly fine and homogeneous. It is plausible that this fine and uniform dispersion of carbide phase could play a vital role in reducing localized stress concentration, thereby leading to more stable cutting conditions, including lower tool wear. Nonetheless, these refined secondary carbides could also facilitate better machinability owing to higher enhanced inherent hardness and wear resistance. In contrast, Figs. 1(c) and (d) present the microstructural

Table 1 Chemical composition of workpieces.

Chemical Composition (DC53 Steel)								
	C%	Cr %	Si %	Mn %	*P* %	S %	Mo %	V%
Workpiece	0.94	7.60	0.97	0.39	0.02	0.003	1.90	0.14
Standard[25]	0.96	8.12	0.95	0.38	0.02	0.005	2.07	0.17
Chemical Composition (D2 Steel)								
	C %	**Cr %**	**Si %**	**Mn%**	**P %**	**S %**	**Mo %**	**Fe %**
Workpiece	**1.51**	**15.3**	**0.42**	**0.37**	0.05	0.02	1.34	Balance
Standard[26]	**1.50**	**12.0**	**0.30**	**0.45**	0.03	0.03	0.90	Balance
Specifications	DC53 Steel (6 circular plates of 152 mm diameter and 12 mm thickness)							
	D2 Steel (2 rectangular plates with 254 mm length, 254 mm width, and 12 mm thickness)							
Hardness (HRC)	28 HRC for both D2 and DC 53 steel							

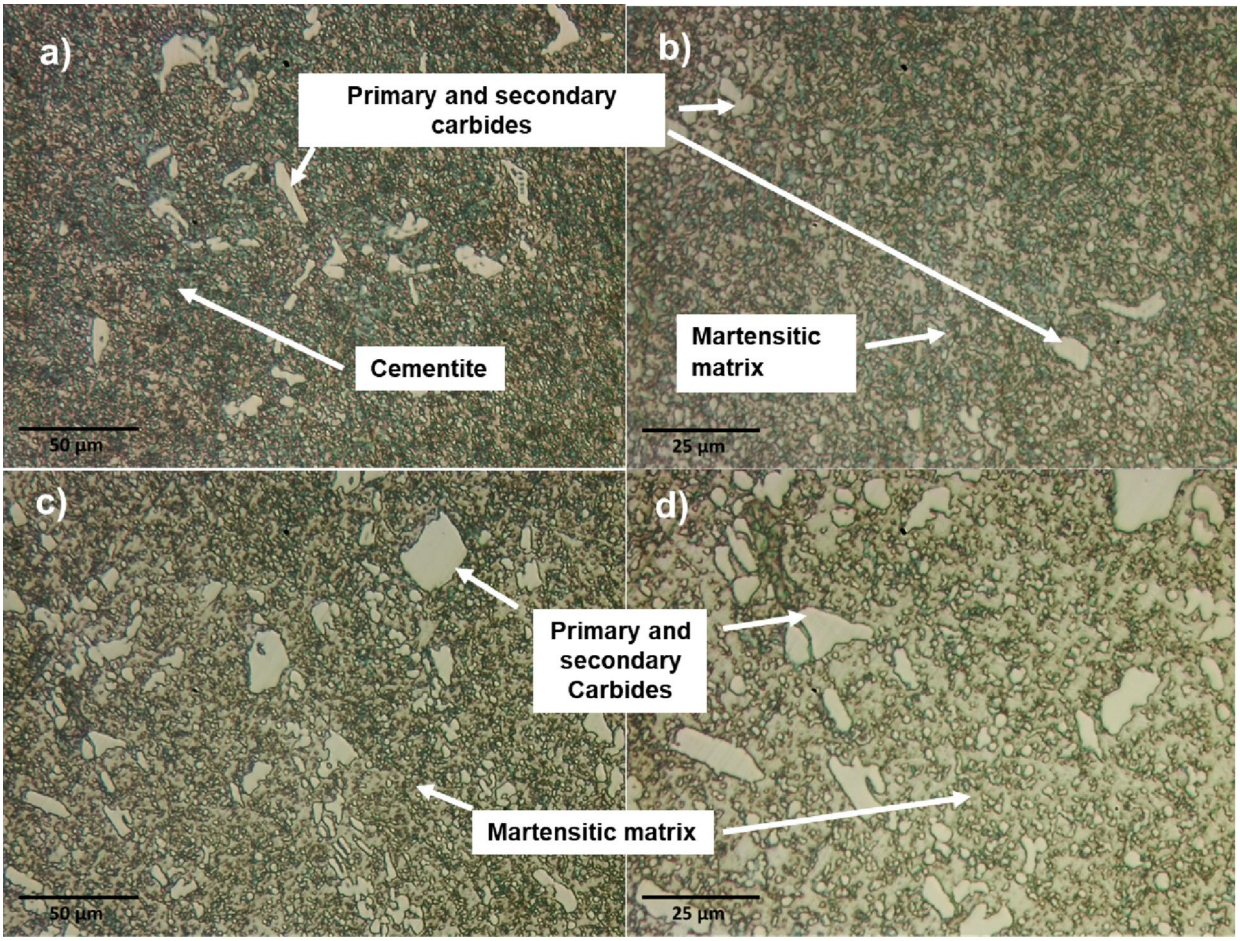

Fig. 1 Microstructural analysis of DC 53 steel, (**a**) at resolution of 200X, (**b**) 500X, and microstructural analysis of D2 steel, (**c**) at 200X, (**d**) 500X.

features of the D2 steel workpiece, which consists mainly of a martensitic matrix with primary and secondary carbide phases. However, when compared to DC53 steel, the D2 steel workpiece exhibits relatively larger, coarser, and more irregular carbide particles distributed throughout the matrix.

The process parameters were chosen based on the values established in previous studies[27–29] for drilling steel with carbide tools under dry conditions. This choice was made because the different tool materials have distinct operating regimes. Since the cutting tools being evaluated are carbide-based, it is rational to select operating

Table 2 Details of work-piece and cutting conditions employed.

Particulars	Details
Cutting speed (m/min)	20 m/min (455 rpm) and 30 m/min (682 rpm)
Feed rate (mm/rev)	0.05, 0.075, and 0.10 mm/rev
Cutting conditions	Dry

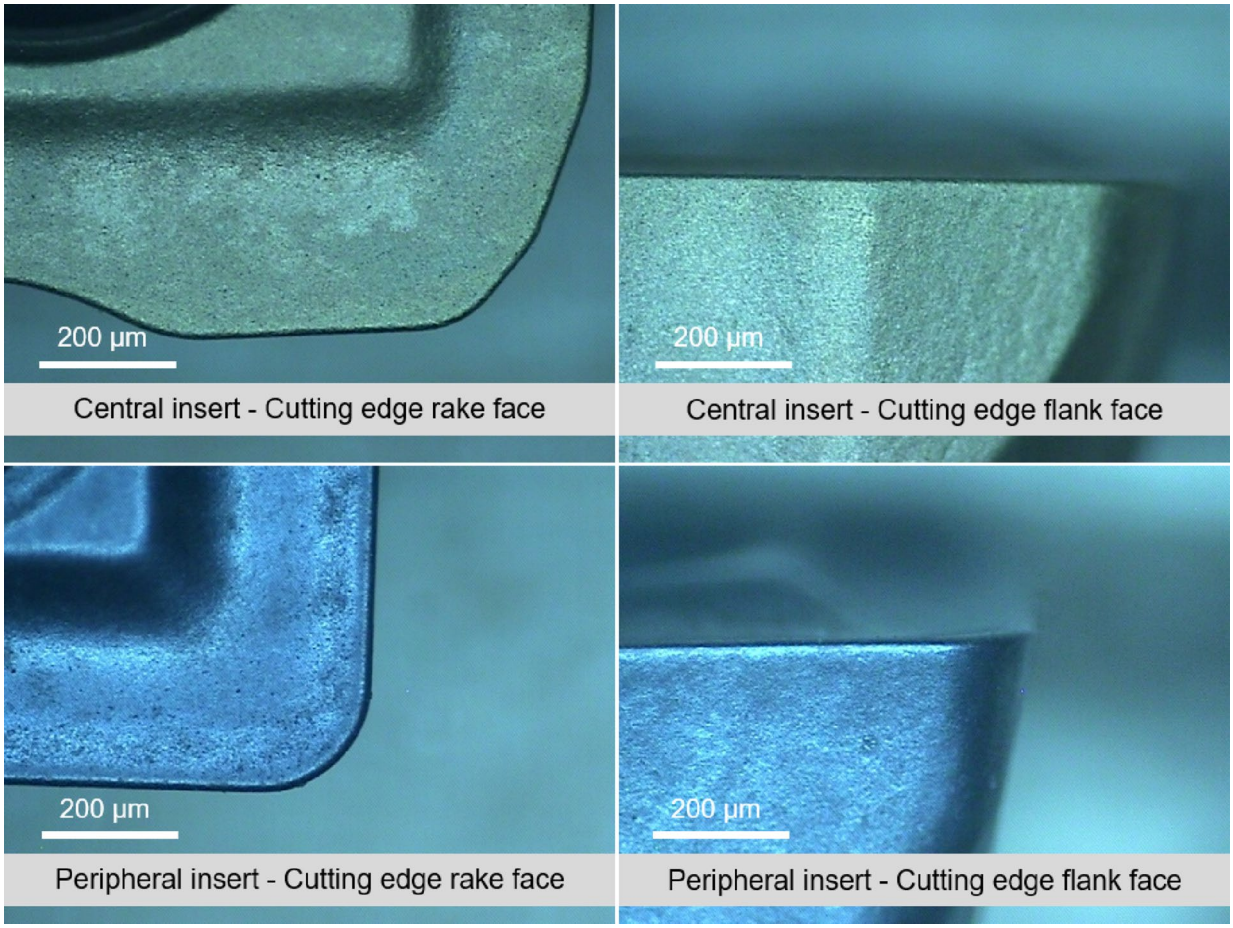

Fig. 2 Flank & rake faces of unworn central and peripheral insert.

parameters from the literature where carbide tooling was assessed for meaningful comparison. The cutting parameters employed are summarized in Table 2.

A indexable tool holder (ISO: 880-D1400L20-03, Ø14 mm) was employed for drilling. Compared with conventional solid carbide twist drills, indexable drills offer several practical advantages for industrial applications. Only the worn inserts require replacement after tool life is reached, significantly reducing tooling cost, machine downtime, and tool change time. In addition, their wider chip evacuation channels improve chip removal, reducing the likelihood of chip clogging and associated tool damage. Indexable drills accommodate two cutting inserts (central and peripheral insert) that simultaneously participate in the drilling operation. Figure 2 illustrates the flank and rake faces of the unused central stepped insert and peripheral wiper insert prior to machining.

The peripheral insert used during this study (ISO: 880-02 02 W05H-P-LM 4344) consisted of a carbide substrate with wiper-edge technology, an LM chip breaker (the schematic of the LM chip-breaker (CB) is shown in Fig. 3; Table 3), a 12.5° rake angle, and a PVD-TiAlN coating. Whereas the central insert (ISO: 880-02 02 04 H-C-LM 1044) featured a carbide substrate with stepped-edge technology, an LM chip-breaker, a 12.5° rake angle, and a PVD–TiAlN coating.

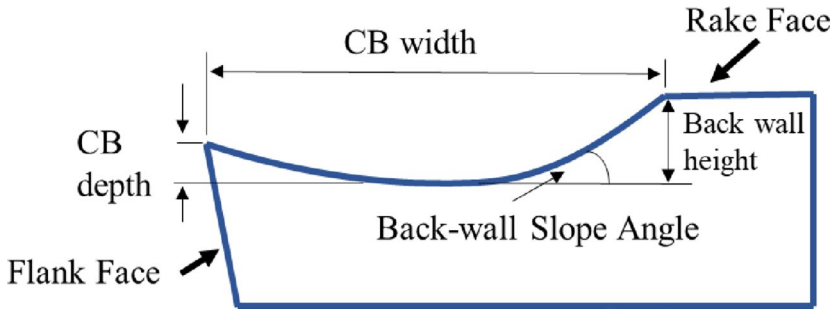

Fig. 3 Chip-Breaker (CB) design.

Table 3 Chip-breaker details.

Wiper inserts chip-breaker	Details
LM	Chip Breaker Width: 1000 µm, CB depth: 65 µm, back-wall height (BH): 210 µm, and slope angle (BS): 30 degrees

A full factorial experimental design consisting of 12 experimental runs (2 × 2 × 3) was conducted using two workpiece materials (DC53 and D2 steel), two cutting speeds (20 and 30 m/min), and three feed rates (0.05, 0.075, and 0.10 mm/rev). The complete experimental setup and test array are shown in Fig. 4; Table 4, respectively. All the tests were repeated twice to check the repeatability of the experiments, and the average values were used for further analysis.

The study employed a Denford VMC 1300 Pro, a 3-axis CNC milling machine characterized by a spindle speed of up to 6000 rpm and a feed rate of 5000 mm/min. In each test, ten holes were drilled; each hole was drilled with a thickness of 12 mm, resulting in a total machined thickness of 120 mm, as 10 holes were drilled. Furthermore, the holes were drilled consecutively under identical machining conditions without any peck strategy and no tool reconditioning between holes, which implies that each time new insert was used. The 4 K Digital Microscope (ZONHMAI: C011607H) with 48 Megapixel resolution and 1–150× zoom capability was used to perform measurements that were analyzed through image-view software running on a PC for image acquisition, tool wear analysis, and diametric error measurement. Furthermore, flank wear measurements were performed at 70× magnification. Flank wear was selected as the primary tool wear indicator because it is the most widely accepted criterion for evaluating tool wear and tool life in machining studies. It directly influences machining accuracy, surface quality, and tool performance, making it a reliable indicator of tool degradation under the present machining conditions[30]. The measurements were carried out following the methodology commonly adopted in previous studies for evaluating tool flank wear under similar machining conditions[31]. Conversely, the exit burr height of the holes was measured using a coordinate measuring machine (CMM: CE450DV). Surface roughness measurements were performed using a Mitutoyo (SJ-210) tester by mounting the workpiece vertically to facilitate probe access inside the drilled holes, as shown in Fig. 4d. Measurements were taken along the axial direction with an evaluation length of 4.0 mm and a cut-off length of 0.80 mm. For all tests, four readings were taken at different points after indexing the workpiece. Specifically, for circular specimens (DC53 Steel), measurements were obtained at angular positions of 0°, 90°, 180°, and 270°, while for rectangular specimens (D2 Steel), measurements were taken along both length and width orientations, and their averages are reported herein. Furthermore, a thermal imager camera, Testo 868, with a range of 0 to + 650 °C, was employed to measure the machining temperature. To ensure measurement accuracy, the surface emissivity was set to 0.95. The thermal imager was

https://doi.org/10.1038/s41598-026-78568-1

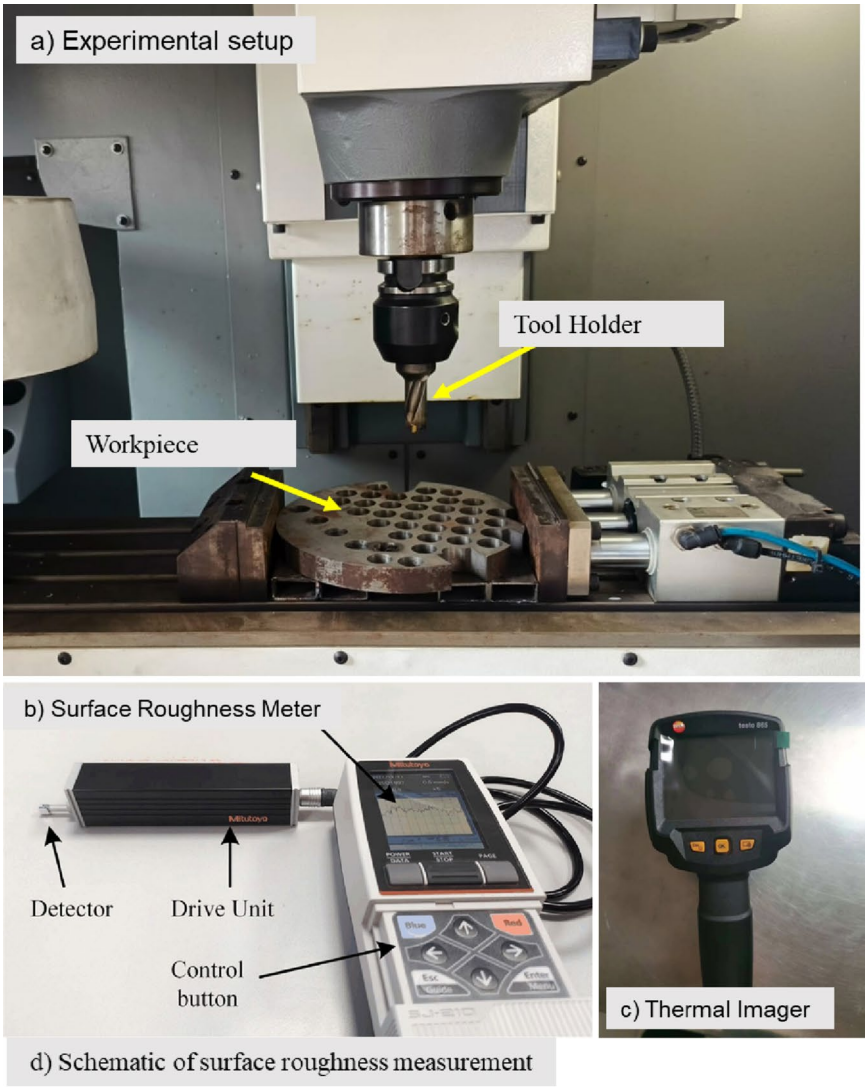

Fig. 4 (**a**) Experimental setup, (**b**) Surface roughness meter, (**c**) Thermal imager camera, (**d**) schematic of surface roughness measurement.

Table 4 Design of experiments.

Test no.	Workpieces	Cutting speed m/min	Feed rate (mm/rev)
1	D2 Steel	20 (455 rpm)	0.05
2	D2 Steel	20 (455 rpm)	0.075
3	D2 Steel	20 (455 rpm)	0.10
4	D2 Steel	30 (682 rpm)	0.05
5	D2 Steel	30 (682 rpm)	0.075
6	D2 Steel	30 (682 rpm)	0.10
7	DC53 Steel	20 (455 rpm)	0.05
8	DC53 Steel	20 (455 rpm)	0.075
9	DC53 Steel	20 (455 rpm)	0.10
10	DC53 Steel	30 (682 rpm)	0.05
11	DC53 Steel	30 (682 rpm)	0.075
12	DC53 Steel	30 (682 rpm)	0.10

positioned at a distance of 200 mm from the machining surface, with a 0° orientation relative to the workpiece surface, and the direct line of sight was consistently maintained to minimize angular measurement deviations. These experimental conditions constitute the measurement protocol followed in this study and are consistent with the procedure reported in the referenced work[32]. The SEM model (JEOL 6060) examined the chosen inserts together with workpiece samples to study tool wear mechanisms, surface damage, and burr formation in detail. The morphology of the cutting chips was also analyzed using SEM. All the tests were repeated twice to check the repeatability, and average values are reported herein.

Previous studies have demonstrated the effectiveness of entropy-weighted TOPSIS or similar multi-objective optimization techniques for evaluating machining performance involving multiple and often conflicting quality characteristics, such as surface roughness, diametric error, tool wear, and cutting temperature[33–37]. Following this approach, an integrated hole quality assessment model is proposed using Entropy-weighted TOPSIS ranking methodology. First of all, normalization of the data is conducted, since all responses are smaller the better; therefore, this formula is used for normalization;

$$Y_{ij}^{*} = \frac{Ymax - Y_{ij}}{Ymax - Ymin} \tag{1}$$

After that, the probability matrix was formulated by using this formula;

$$P_{ij} = \frac{Y_{ij}^{*}}{\sum_{i=1}^{m} Y_{ij}^{*}} \tag{2}$$

Following the probability matrix, entropy, degree of diversification, and entropy weights, abbreviated as E_j ,dj ,w_j, respectively, are calculated using the following formulas;

$$E_j = -\frac{1}{\ln(m)} \sum_{i=1}^{m} P_{ij} ln(P_{ij}) \tag{3}$$

$$dj = I - E_j \tag{4}$$

$$w_j = \frac{d_j}{\sum_{j=1}^{n} d_j} \tag{5}$$

A consolidated Table 5 showing entropy, degree of diversification, and weights of each response is given here;

So the roughness of the drill received the highest weight with a value of ~0.313 due to larger variations associated with this response. Machining temperature (MT), Exit burr height (EBH), diametric error (DE), and tool wear (TW) were correspondingly assigned weights with values ~0.186, ~0.179, ~0.177, and ~0.146, respectively.

Table 5 Entropy weights for each response.

Response	E_j	dj	w_j
Tool wear	0.9306	0.0694	0.1457
Surface roughness	0.8511	0.1489	0.3127
Diametric error	0.9106	0.0840	0.1766
Temperature	0.9113	0.0887	0.1864
Exit burr height	0.9149	0.0851	0.1787

For holistic machining assessment of these indexable drilling inserts considering tool wear and hole integrity attributes together, a model based on entropy weights was developed, which is given as;

$$IHII = 0.146\,TW^* + 0.313\,Ra^* + 0.177\,DE^* + 0.186\,MT^* + 0.179\,EBH^* \tag{6}$$

Where TW*, Ra*, DE* and MT* and EBH* are normalized values of tool wear, surface roughness, diametric error, machining temperature and exit bur height respectively and corresponding weights were assigned as per entropy weighted method. The suggested hole integrity index was used for overall comprehensive drilling assessment of these trials. Integrated hole integrity index (IHII) is developed which simultaneously combines all output responses into a single quantitative performance indicator for holistic drilling performance in the current scenario. The value of IHII varies between 'Zero (0)' to 'One (1)', with '0' showing the poor drilling conditions and the higher and closer to '1' value describes the best drilling condition. Finally, graphs were plotted between this performance metric against tool wear is explained.

TOPSIS analysis was conducted subsequently to determine the closeness coefficient, and the experimental array was ranked accordingly. For TOPSIS analysis, the same entropy weights and min. max. methodology was employed. First of all, v_{ij} value was calculated from the entropy weights, w_j, and the normalized value y_{ij}^*;

$$v_{ij} = w_j y_{ij}^* \tag{7}$$

Then the positive ideal solution $A^+$was determined which is given below;

$$A^+ = \{0.146,\ 0.313,\ 0.177,\ 0.186,\ 0.179\} \tag{8}$$

Then the negative ideal solution is;

$$A^- = \{0,0,0,0,0\} \tag{9}$$

Separations from ideal solution is;

$$Si^+ = \sqrt{\sum {}_{j=1}^{n}\left(v_{ij} - A_j^+\right)^2} \tag{10}$$

Separations from negative ideal solutions is;

$$Si^- = \sqrt{\sum {}_{j=1}^{n}\left(v_{ij} - A_j^-\right)^2} \tag{11}$$

Closeness coefficient way

$$CC_i = \frac{S_i^-}{S_i^+ + S_i^-} \tag{12}$$

Then on the basis of this, ranking was determined and graph was plotted.

Results and discussion

Tool wear

Drilling tests on D2 and DC53 steels were performed, and tool wear was measured after each test, which involved drilling ten holes or 120 mm machining length. Figure 5 shows the results of the tool wear experiments. In all the tests, D2 steel showed less tool wear than DC53 steel. In Test 1, the least wear observed on D2 steel was 49 µm, which occurred at a cutting speed of 20 m/min and a feed rate of 0.05 mm/rev. However, using the same cutting speed and feed rate, the DC53 showed approximately the equivalent flank wear, measuring 50 µm. It was also observed that the effect of cutting speed and feed rate has a direct relation with the flank wear, such that with an increase in cutting speed or feed rate, the flank wear increased for both the steels. For D2 steel, at 20 m/min, when the feed rate was increased from 0.05 mm/rev to 0.10 mm/rev, the tool wear increased from 49 µm to 51 µm (6.25% increase). Whereas for DC53 steel, this increase was a bit higher, such that for the same cutting speed and the same increase in feed rate, the flank wear jumped from 50 µm to 66 µm, which is a 32% increase in wear. Similarly, when the feed rate was kept constant (0.075 mm/rev) with the increase in cutting speed from 20 m/min to 30 m/min, flank wear when drilling D2 steel was elevated from 50 µm to 56 µm (12% increase). In contrast, for DC53 steel, when machined under the same conditions, the increase in flank wear was higher, going from 59 µm to 79 µm, which is a 34% increase in the flank wear.

The highest tool wear values were consistently observed for DC53 steel, particularly at the combination of high cutting speed and feed rate. The highest value of 82 µm occurred during Test 12 when the machine operated at 30 m/min with 0.10 mm/rev. This is 47% higher than the highest value of wear observed in Test 6 conducted on D2 steel. This indicates that for all the tests, DC53 steel causes higher tool wear than D2 steel with the same cutting conditions. This can be attributed to the microstructural difference between D2 and DC 53 steels. For DC53 steel, the presence of finely distributed carbides plays a crucial role in the tool wear during machining processes. Despite sharing identical hardness levels, D2 and DC53 steels possess distinct carbide structures. D2 steel is characterized by larger, coarser carbides, while DC53 features a finer, more uniform distribution. Consequently, even though individual D2 carbides may be inherently more abrasive, their discontinuous interaction with the cutting

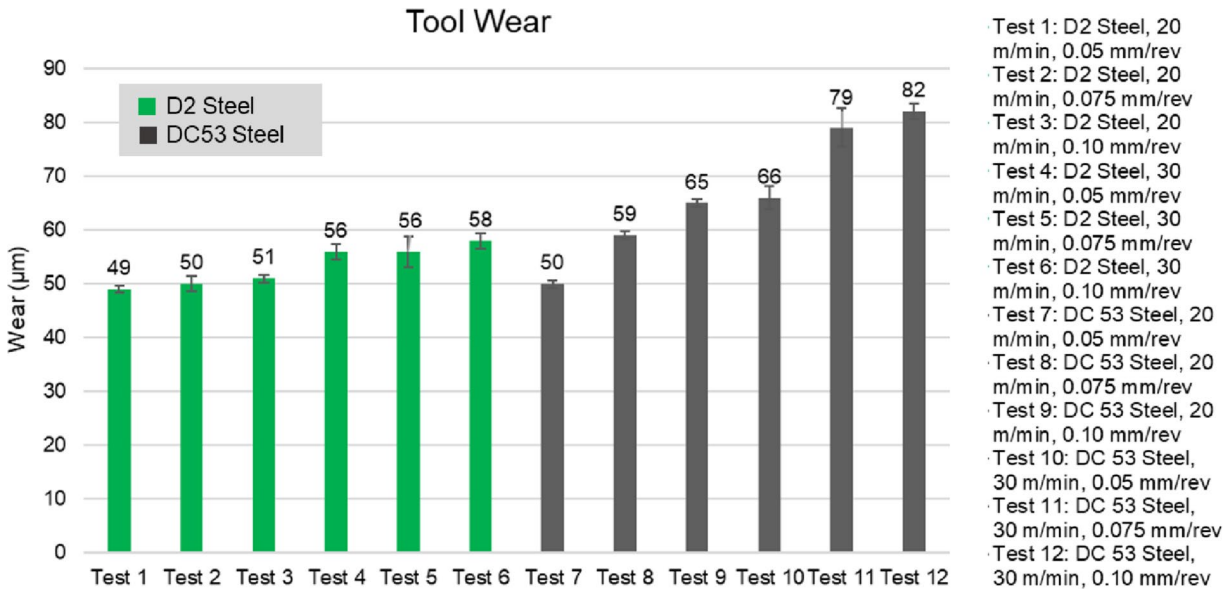

Fig. 5 Tool Wear for Each Test.

edge results in less wear. Conversely, the homogenous, fine carbide dispersion in DC53 facilitates a steadier abrasive contact during drilling operations, ultimately causing increased tool wear compared to D2 steel.

Figure 6 shows the wear behavior of the central stepped insert during the experiments. Compared with the peripheral wiper insert, the central stepped insert exhibited substantially lower wear under all cutting conditions. This behavior is attributed to the lower cutting speed and reduced heat generation near the drill center, resulting in less severe wear[38]. Consequently, the peripheral wiper insert governed the overall tool life and had a greater influence on the machined hole surface. Therefore, the present study primarily focuses on the wear behavior of the peripheral wiper insert, while the wear of the central stepped insert is briefly discussed for completeness.

Optical micrographs for selective tests are shown in Figs. 7a) – f). These images were taken at the end of each test (after drilling 10 holes). There was no sign of a catastrophic fracture in any of the tests. However, it was observed that the main cause of wear is gradual wear, with minor chipping being seen only in Test 5, see Fig. 7c). With one exception, as stated, flank wear was uniform in general. In contrast, Figs. 7d) – f) show the wear of the wiper insert when drilling DC53 steel. These inserts showed higher wear as compared to those that were used in D2 steel. A minor buildup edge is also visible in Fig. 7e). Also, with an increase in cutting speed and feed rate, an increase in the wear on micrographs is clearly visible; this result is in conformity with the quantitative results of tool wear, which are already discussed in the previous section.

Chips were collected across all experimental conditions. Thickness was evaluated using an optical microscope at three random points per chip, with reported figures representing the mean of twenty chips per condition. Quantitative measurements revealed that D2 produced chips with an average thickness of 58 ± 02 µm, while DC53 resulted in an average of 60 ± 05 µm. Despite comparable thicknesses under similar conditions, morphology differed significantly. D2 typically yielded segmented, fractured chips, whereas DC53 formed continuous ribbons, as depicted in Figs. 7g–j. These differences arise from the unique microstructures of the steels: the coarse, heterogeneous carbides in D2 serve as stress concentrators that foster crack initiation and propagation in the primary shear zone, driving chip segmentation. Conversely, the fine, uniform carbides in DC53 foster a stable shear process, resulting in continuous chip formation. It is important to note that continuous chips do not indicate lower tool wear; rather, DC53's uniform carbides provide consistent abrasive contact with the cutting edge, leading to sustained wear. In contrast, D2's coarse carbides result in localized fracturing and non-uniform abrasive engagement. Thus, chip morphology and tool wear are driven by independent mechanisms and are not directly correlated.

Surface integrity

Surface roughness (Ra)

The surface roughness (Ra) data, as shown in Fig. 8, from drilling D2 and DC53 steels, demonstrates the gradual impact of cutting parameters and tool-workpiece interaction on surface roughness as the number of drilled holes

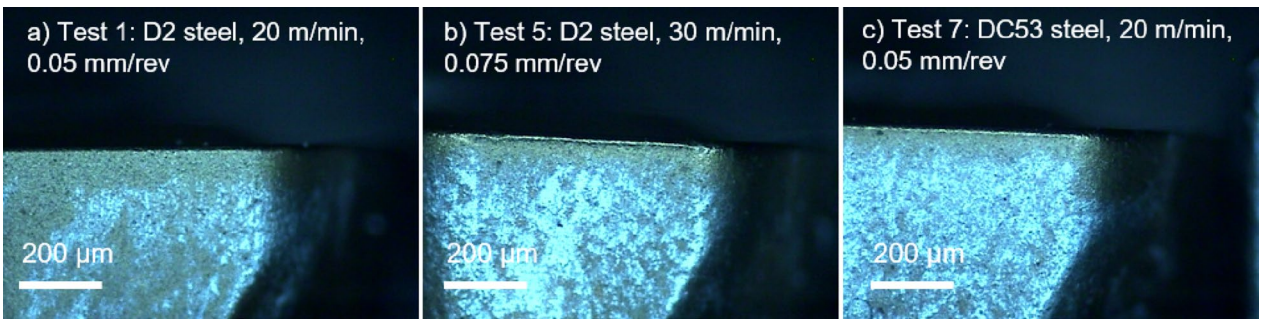

Fig. 6 Tool wear of central step inserts for Test 1, 5 and 7.

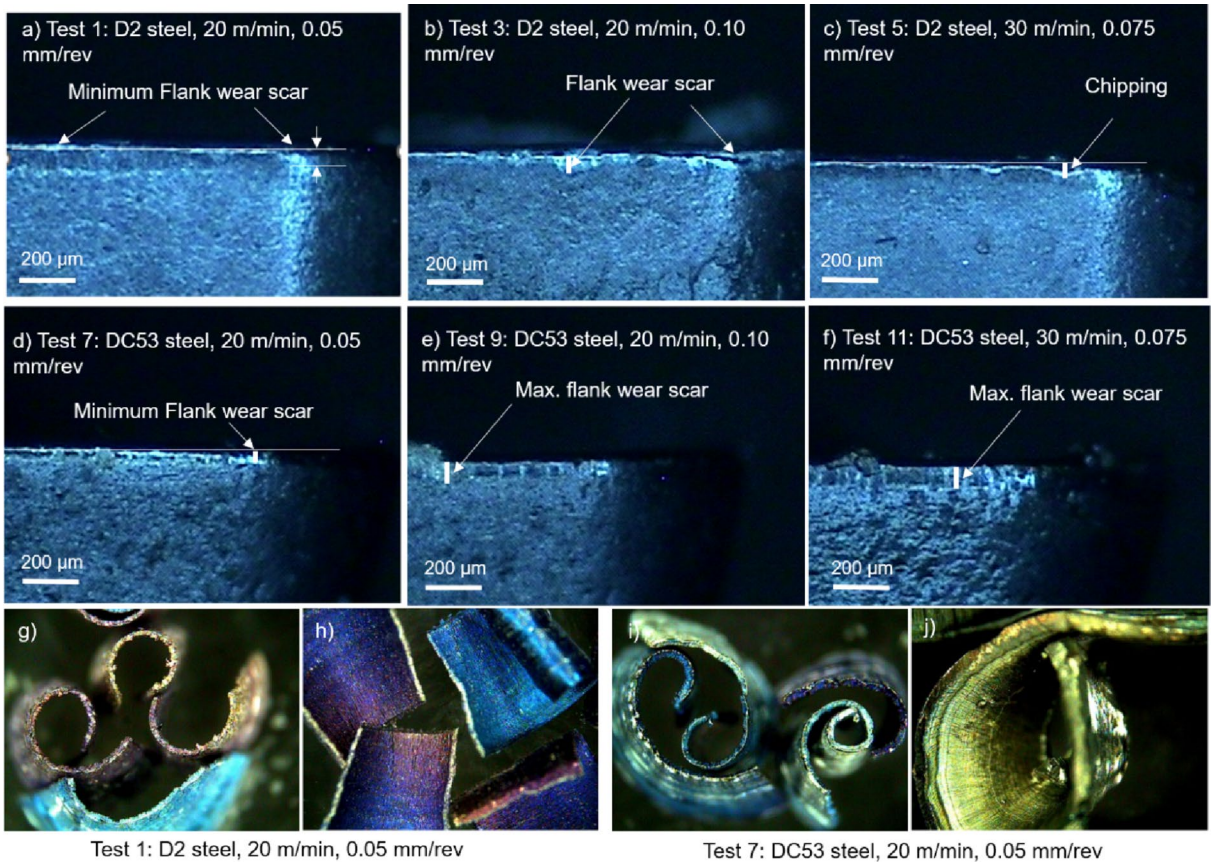

Fig. 7 (**a**), (**b**), (**c**), (**d**), (**e**), (**f**) Tool Wear Progression of Wiper Inserts, cutting chips for (**g**), (**h**) Test 1 (D2 steel, 20 m/min, 0.05 mm/rev), (**i**), (**j**) for Test 7 (DC53 steel, 20 m/min, 0.05 mm/rev).

increases. In general, the surface roughness of DC53 steel was consistently higher than that of D2 steel. In the case of D2 steel, the lowest surface roughness of 1.0 µm was observed in Test 1 at the start of cutting, which increased to 1.6 µm after drilling 10 holes. The highest Ra value for the DC53 steel was observed in Test 6 (30 m/min, 0.10 mm/rev), which increased from 3.6 µm to 4.8 µm for the last hole, which is a 33% increase. In the case of DC53 steel, all the tests showed higher Ra values as compared to D2 steel. The minimum Ra of 1.9 µm was observed in Test 7 (20 m/min, 0.05 mm/rev) when cutting DC 53 steel, which increased to 2.8 µm for the last hole.

The surface roughness tests revealed that Ra values of DC53 steel exceeded those of D2 steel. This can be attributed to the rapid flank wear and increased cutting temperatures encountered during the machining of DC53, which intensifies the tool–workpiece interaction and encourages rubbing and ploughing actions. Moreover, the continuous chip formation linked to the fine microstructure of DC53 also intensified adhesive interactions at the tool-chip interface, causing material smearing and surface deformation. Additionally, the consistent micro-abrasive effect of fine carbides led to uniform surface scratching. Conversely, the segmented chip formation and lower average cutting temperatures in D2 steel minimized the extended contact and friction, resulting in relatively lower Ra values. Furthermore, the results highlight that surface roughness increases with both feed rate and cutting speed, consistent with the observed thermal behavior. The results for surface roughness are consistent with the previous literature, such that, generally, an increase in feed rate has been found to significantly increase surface roughness. This is due to the greater cusps height of the machined surface associated with elevated feed rate values, leading to a poor surface finish[39,40]. Compared with the work of Yaka et al.[41], who reported a minimum surface roughness of 1.53 µm during flood-cooled drilling of D2 steel using TiN-coated carbide drills, the present study achieved a minimum surface roughness of 0.9 µm under dry drilling conditions. This corresponds to

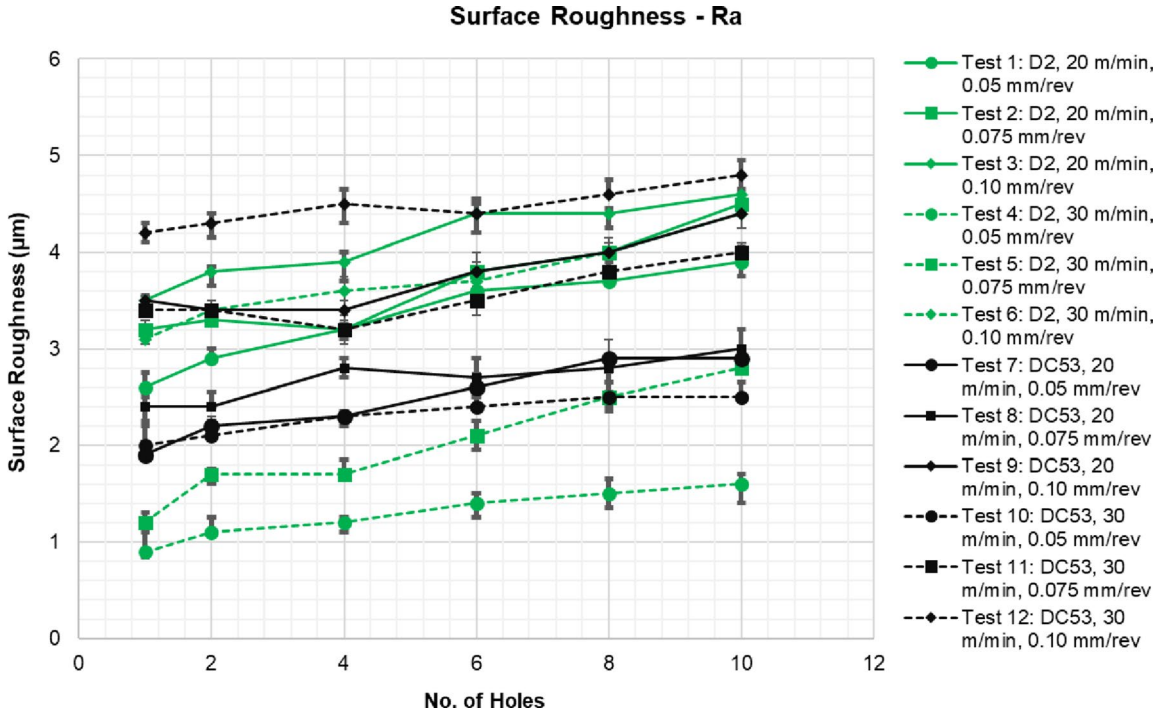

Fig. 8 Variation of surface roughness (Ra) with the number of holes during drilling.

a 34.6% improvement in surface finish, highlighting the effectiveness of the proposed indexable drill configuration in enhancing hole quality while eliminating the need for coolant.

Surface damage

Figure 9 shows scanning electron microscopy (SEM) images of drilled holes in D2 steel, taken under two different machining conditions: Test 1 (20 m/min, 0.05 mm/rev) and Test 3 (20 m/min, 0.10 mm/rev). The micrographs clearly demonstrate the impact of feed rate on the surface morphology and damage characteristics. UnderTest 1 conditions, the machined surface typically exhibited material side flow that is evident from the plastically deformed and elongated materials layer oriented parallel to the feed. From the viewpoint of machining, this phenomenon is generally attributed to the localized plastic deformation generated from the prolonged interaction between the cutting edge and workpiece material at lower feed[42–44]. Conversely, surface features generated under Test 3 conditions with a higher feed rate (0.10 mm/rev) exhibited severe surface tearing, adhered material deposits, and the presence of micro-particles attached to the machined surface. It is of general belief that at a higher feed rate, the undeformed chip thickness and cutting forces result in elevated friction and temperature at the tool-workpiece interface. Consequently, under these typical scenarios, the adhesion wear phenomenon becomes stronger, which mainly arises from the disintegration of workpiece material that could adhere to the cutting insert due to thermo-mechanical loading and subsequently detach, leading to adhered layers and damaged regions on the freshly machined surface. Nevertheless, as mentioned in Fig. 1, the repeated interaction of the hard carbide phase in D2 steel and the cutting edge could further accelerate localized stress concentration, promoting micro-fracture and tearing of the surface layer as seen in Fig. 7. Similar results are observed in the literature, where higher feed rates lead to elevated temperatures; thus, they promote both adhesion and tearing[45,46]. In short, the SEM observation corroborated that increasing the feed rate substantially alters the surface damage mechanism from dominant plastic side flow at lower feed rates to severe adhesion at higher feed rates.

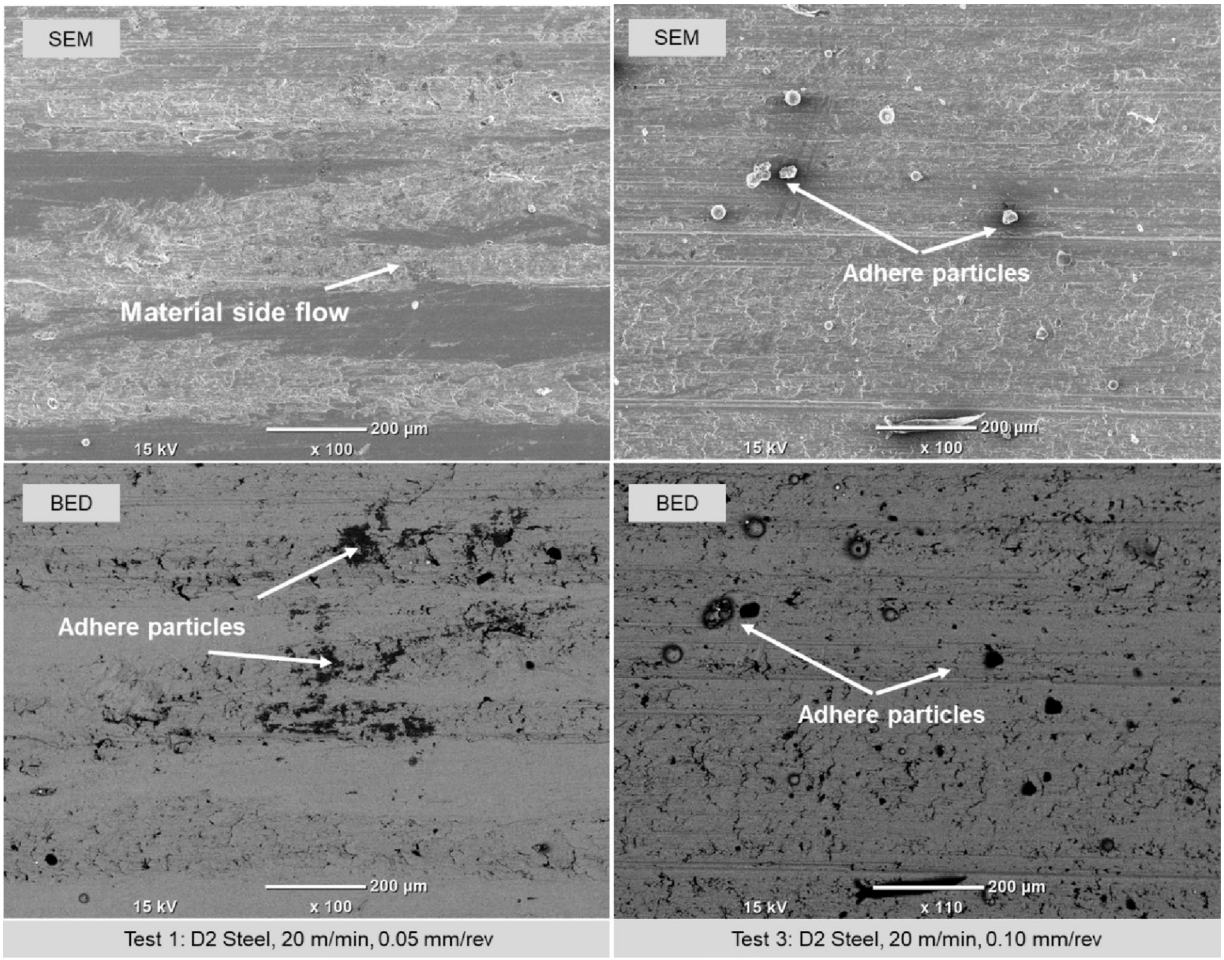

Fig. 9 Surface damage analysis observed in Test 1 and Test 3.

Moreover, SEM analysis for the test conducted on the DC 53 steel is shown in Fig. 10. Test 7 (20 m/min, 0.05 mm/rev) and Test 9 (20 m/min, 0.10 mm/rev) showed surface damage on DC53 steel when the feed rate is increased from 0.05 m/rev to 0.10 mm/rev at a constant cutting speed of 20 m/min. For Test 7 conducted at 0.05 mm/rev, material side flow and minor adhered particles are clearly visible. The adhesion shows that the workpiece material is welded to the newly machined surface owing to strong frictional forces and high temperature. At the same time, the material side flow observed during this test suggests that the surface layer has undergone plastic deformation. Overall, the SEM analysis for Test 9, which used a feed rate of 0.10 mm/rev, shows strong material side flow and plastic deformation on the machined surface. Whereas the adhesion of particles is less compared to the previous result, which suggests that a higher feed rate tends to plastically deform the surface rather than cause particle adhesion. When comparing the results of D2 and DC53 steel, it was observed that D2 steel showed lower surface damage as compared to the DC53 steel. This result is also in line with the previously discussed Ra values, where DC53 steel showed higher Ra values compared to its counterpart.

Machining temperature analysis

The recorded machining temperatures for D2 steel and DC53 steel under varying cutting parameters are depicted in Fig. 11. For D2 steel (Tests 1–6), the temperatures ranged from 241 °C to 302 °C. The lowest temperature reading appeared in Test 1 at 241 °C when machining was done at 20 m/min with 0.05 mm/rev. The highest

https://doi.org/10.1038/s41598-026-78568-1

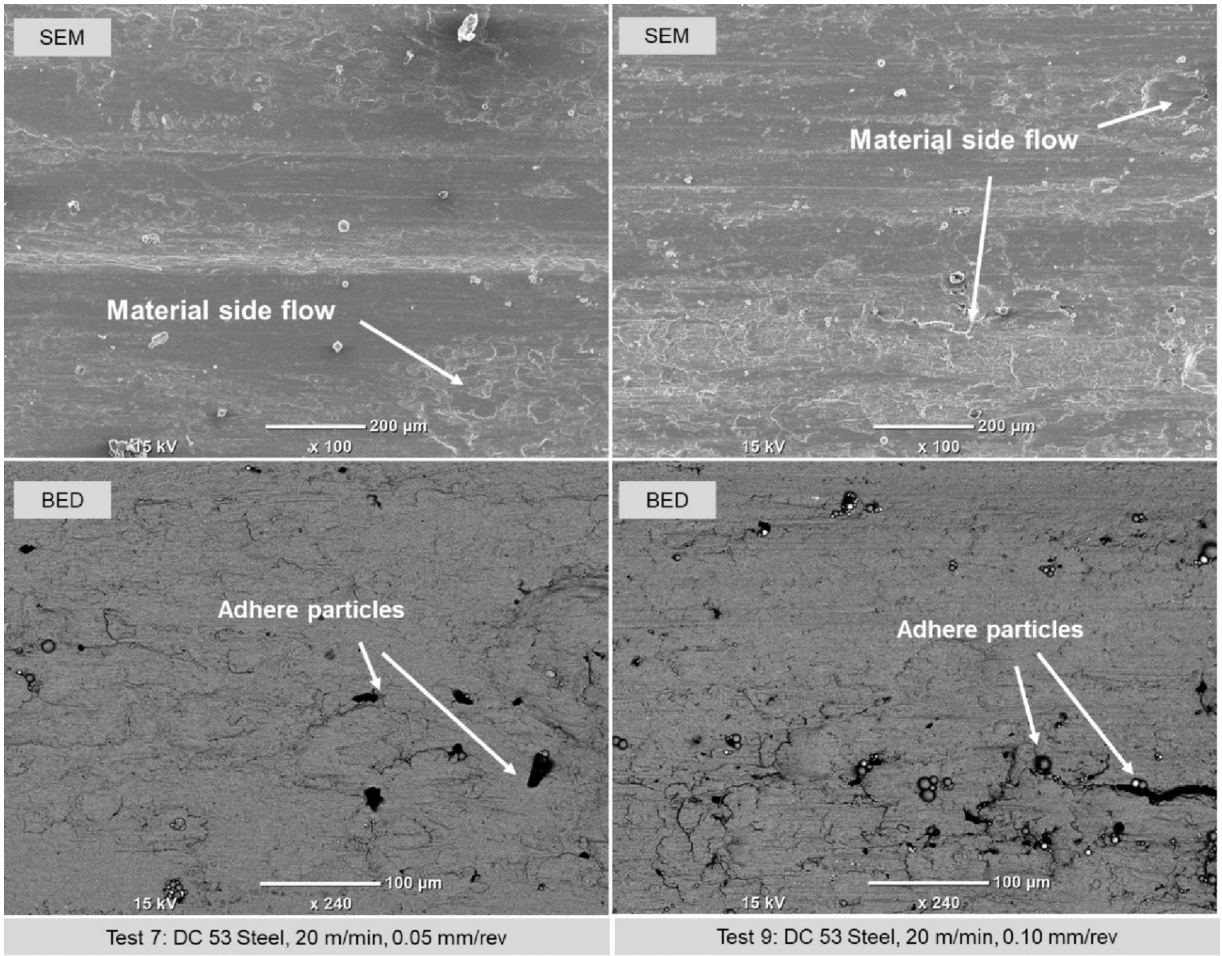

Fig. 10 Surface damage analysis observed in Test 7 and Test 9.

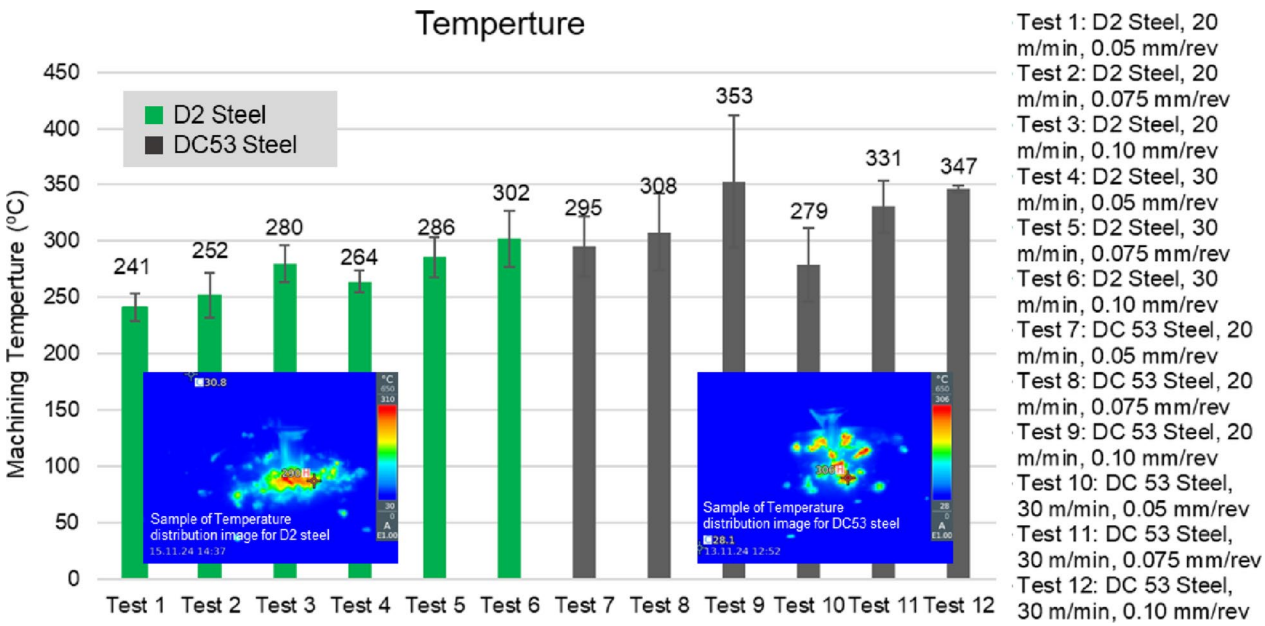

Fig. 11 Comparative analysis of machining temperature under different test conditions.

temperature reading of 302 °C was recorded in Test 6 at a cutting speed of 30 m/min with a 0.10 mm/rev feed rate. The data demonstrate that feed rates and cutting speeds control temperature increases because these variables create a direct relationship between them[47–49].

Similar results were obtained for the DC53 steel; however, the machining temperatures were generally higher than those of D2 steel under comparable cutting conditions, ranging from 279 °C to 353 °C (Test 7–12). The lowest temperature of 279 °C was observed in Test 10 using 30 m/min and 0.05 mm/rev feed rate. However, the highest temperature of 353 °C was recorded in Test 9 at 20 m/min and 0.10 mm/rev. The maximum temperature occurred in Test 9 because the increased feed size induced excessive material deformation, which produced more heat during the cutting process despite utilizing a slower cutting speed. The thermal response of the material changed when the cutting speed reached 30 m/min during Tests 10–12. The temperature reached 347 °C during Test 12 while cutting at 30 m/min with a 0.10 mm/rev feed rate. The DC53 had fine carbides, which were distributed equally, maximizing the tool-chip contact surface area, resulting in frictional heat. Furthermore, as discussed in the previous section, the cutting process of DC53 generates continuous cutting chips, which create an obstacle for heat removal from the tool-work interface. The tool workpiece contact and friction increased because of DC53 flank wear, which caused the tool to reach higher steady-state temperatures. In contrast, the D2 tool experienced better heat dissipation because its uneven carbide distribution led to the development of segmented chips, which produced intermittent cutting action. The tool experienced lower average cutting temperatures because of its carbide distribution pattern.

Diametric error

Figure 12 illustrates the variation in diametric error as a function of the number of holes drilled under varying cutting speed and feed rate conditions. Contrary to the trends observed in surface roughness, the diametric error exhibits a progressive decrease with an increasing number of holes for both materials. The decrease in the diametric error can be attributed to the tool edge wear, which causes a reduction in the drill diameter, which also affects the reduction in the oversize. Furthermore, the low thermal conductivity of workpieces can cause excessive heat

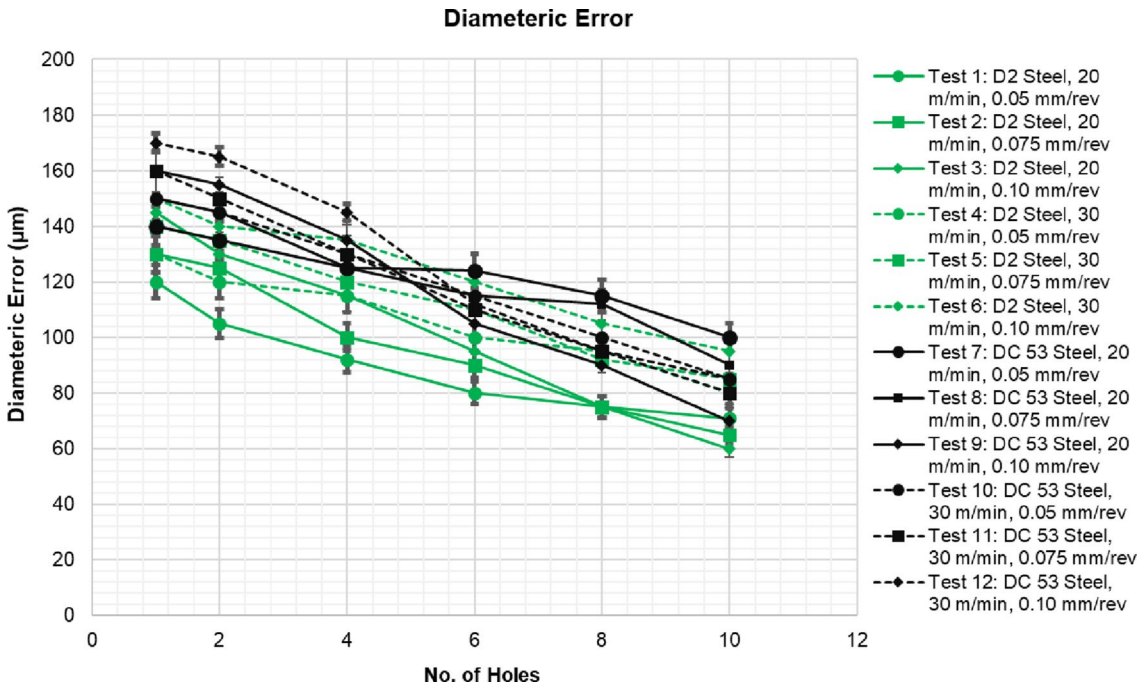

Fig. 12 Variation of diametric error with the number of holes during drilling.

buildup, leading to thermal expansion of the workpiece[50–52]. The diametric error for D2 steel starts at 120–140 µm for the first hole based on feed rate settings before it decreases to 60–70 µm for the following 10 holes. The best results were observed in Test 1 at 20 m/min and 0.05 mm/rev because the diametric error decreased from 120 µm to 63 µm, which resulted in a 48% reduction. The largest decrease in values happened during the initial 4–6 holes before the pattern reached a steady point, which showed no further change.

In the case of DC53 steel, the diametric error measured between 140 and 170 µm during testing with Test 12 (20 m/min, 0.10 mm/rev), showing the highest value of 170 µm at the first hole. The diametric error reached its lowest point at 85–95 µm during the drilling process after drilling 10 holes. The diametric errors from DC53 steel exceeded D2 steel diametric errors by 20–30% under the same cutting conditions. The DC53 drilling process produced high drilling temperatures, which led to an increased thermal expansion of the workpiece and a larger effective cutting diameter. Additionally, the continuous chip formation linked to the refined microstructure of DC53 resulted in an increase in diametric error due to poor chip evacuation. However, the D2 steel contains a dense carbide structure, which enables segmented chip formation and fracture-assisted material removal to achieve better dimensional control and minimize diametric errors.

Burr analysis

Quantitative analysis

Exit burr height analysis for all the tests is shown in Fig. 13. In general, it was observed that with an increase in the number of holes, an increase in the exit burr height was prominent. This indicates that the combined effect of tool wear and increased mechanical and thermal loading influenced the exit burr height[53,54]. For D2 steel, the lowest exit burr height of 175 µm was observed in Test 1 (20 m/min, 0.05 mm/rev), which then increased to 475 µm for the last hole. The highest burr of 290 µm for D2 steel was observed in Test 6, conducted at the highest cutting speed of 30 m/min and feed rate of 0.10 mm/rev, which then increased to 525 µm, showing an 81% increase in the last hole. Previous studies also found the same trend, such that an increase in the cutting speed and

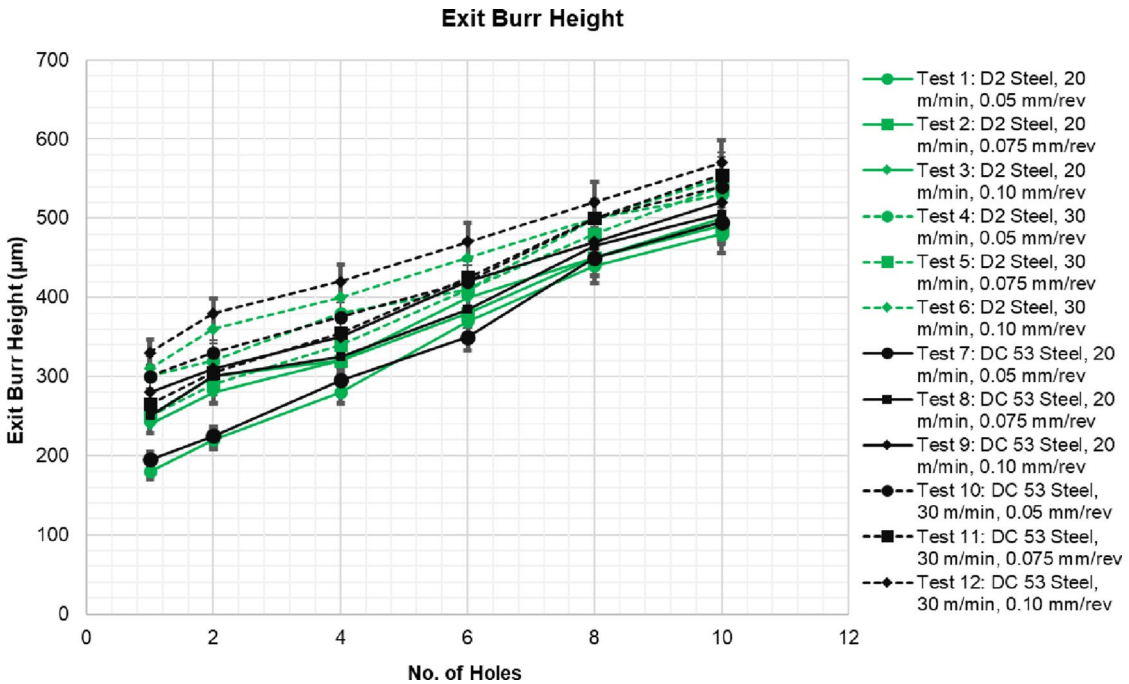

Fig. 13 Variation of exit burr height with the number of holes drilled.

feed rate increases the burr owing to mechanical loading and thermal softening[55,56]. In the case of DC 53 steel, burr height was generally larger than that of the D2 steel. The smallest burr height of 190 µm was observed in Test 7, conducted at the lowest cutting speed of 20 m/min and feed rate of 0.05 mm/rev, which then increased to 490 µm for the last hole, showing a 2-fold increase. This increase in the burr height can be related to the tool wear, as discussed in the tool wear section, where higher tool wear was observed for the DC53 steel. Similar results were observed in[57], where drilling titanium alloys showed comparable behavior for exit burr height. The results confirm that burr formation is strongly influenced by both cutting parameters and the properties of the material. Specifically, higher cutting speeds and feed rates, combined with ductile materials like DC53, lead to the creation of larger burrs. The measured exit burr heights indicate that a secondary deburring operation may be required for applications demanding high edge quality or tight burr tolerance. However, the necessity of deburring ultimately depends on the functional requirements and permissible burr limits of the intended industrial application.

Qualitative analysis

For qualitative analysis, SEM analysis was conducted to provide a better view of the burr at the inlet and exit of the hole. Figure 14 shows the inlet and exit burr generated in Test 1 conducted on D2 steel (20 m/min, 0.05 mm/rev). Minor plastic deformation was observed at the inlet of the hole, which suggests that material is flowing and being smeared. However, the exit section of the hole shows clear signs of fracture, leading to uneven edges and a rough surface. For Test 3, conducted at a higher feed rate of 0.10 mm/rev on D2 steel using 20 m/min of cutting

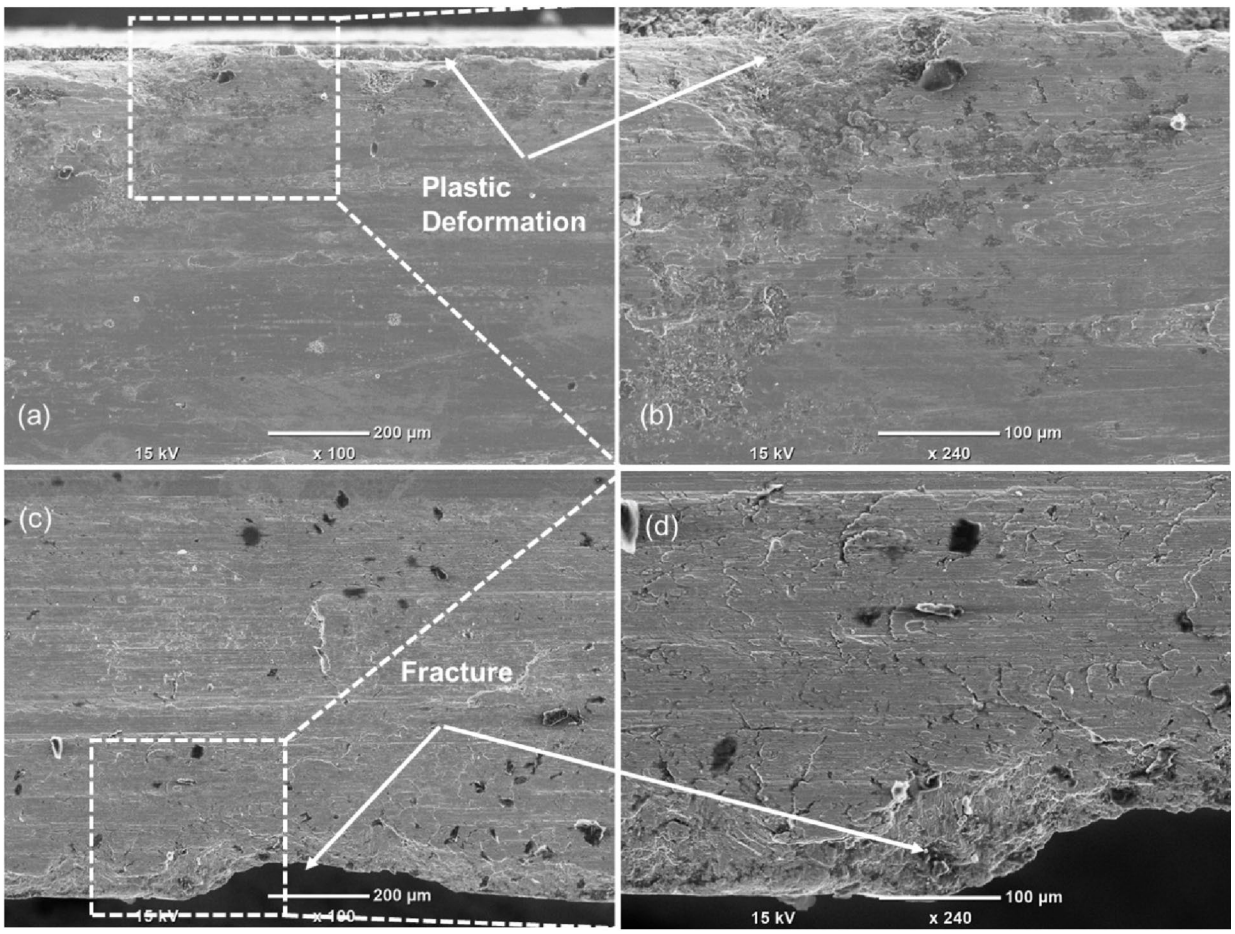

Fig. 14 SEM-based qualitative analysis of hole inlet (**a**, **b**) and exit (**c**, **d**) for Test 1 (D2 Steel, 20 m/min, 0.05 mm/rev).

speed, the inlet and exit burr analysis is shown in Fig. 15. The inlet again shows minor plastic deformation. However, the exit showed rougher edges and fractures.

For DC53 steel, SEM analysis of inlet and exit burrs for Test 7, conducted at the lowest cutting speed and feed rate (20 m/min, 0.05 mm/rev), is shown in Fig. 16. The inlet showed minor plastic deformation, indicating strong material displacement at the entry. However, at the exit, the fracture is more pronounced, with edge breakage confirming that burr formation is governed by the fracture mechanism rather than deformation. The scanning electron microscope (SEM) images in Fig. 17 for Test 9 (DC53 Steel, 20 m/min, 0.10 mm/rev) show plastic deformation on the machined surface. The images demonstrate that material transfer occurred through adhered particles while showing the fracture regions, which are located near the sample edges. The drilling process of Ti-6Al-4 V material produces three distinct mechanical behaviors, which include plastic deformation, adhesive bonding, and brittle material failure. The cutting tool surface quality and its wear pattern result from these operational mechanisms.

The burr formation behavior in this research study depended on both material structure and the thermal and mechanical impacts that occurred during the machining process. The burr height of DC53 steel became higher because its martensitic structure was more refined, and its ductility increased, which allowed the material to deform plastically during the hole exit process. The high machining temperature, together with continuous chip formation, made the exit material softer, which kept the thrust forces active during breakthrough to create burr growth. The DC53 tool showed rapid deterioration, which caused its cutting edge to lose its sharpness and made the material more resistant to cutting, resulting in a severe burr. The D2 steel shows a coarse carbide structure,

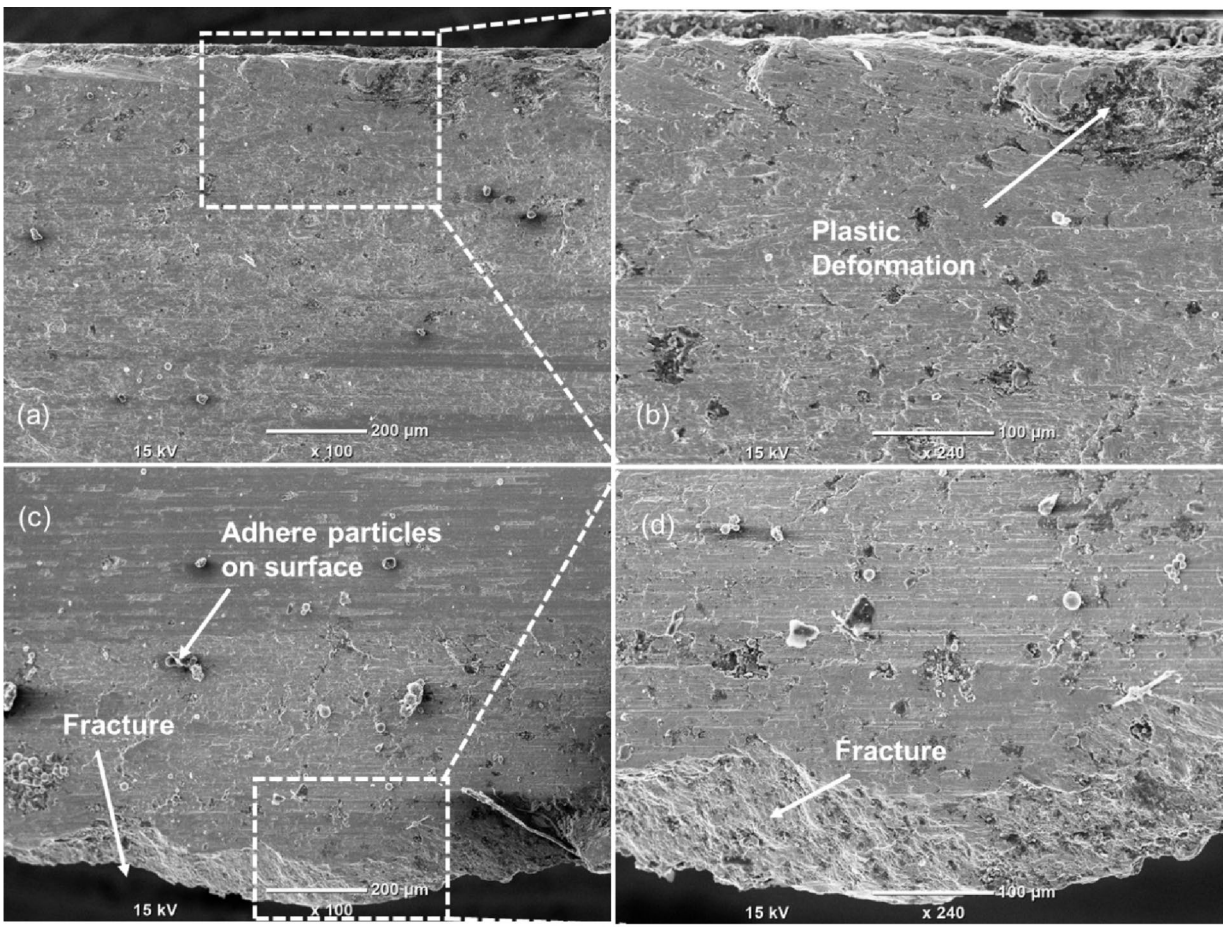

Fig. 15 SEM-based qualitative analysis of hole inlet (**a**, **b**) and exit (**c**, **d**) for Test 3 (D2 Steel, 20 m/min, 0.10 mm/rev).

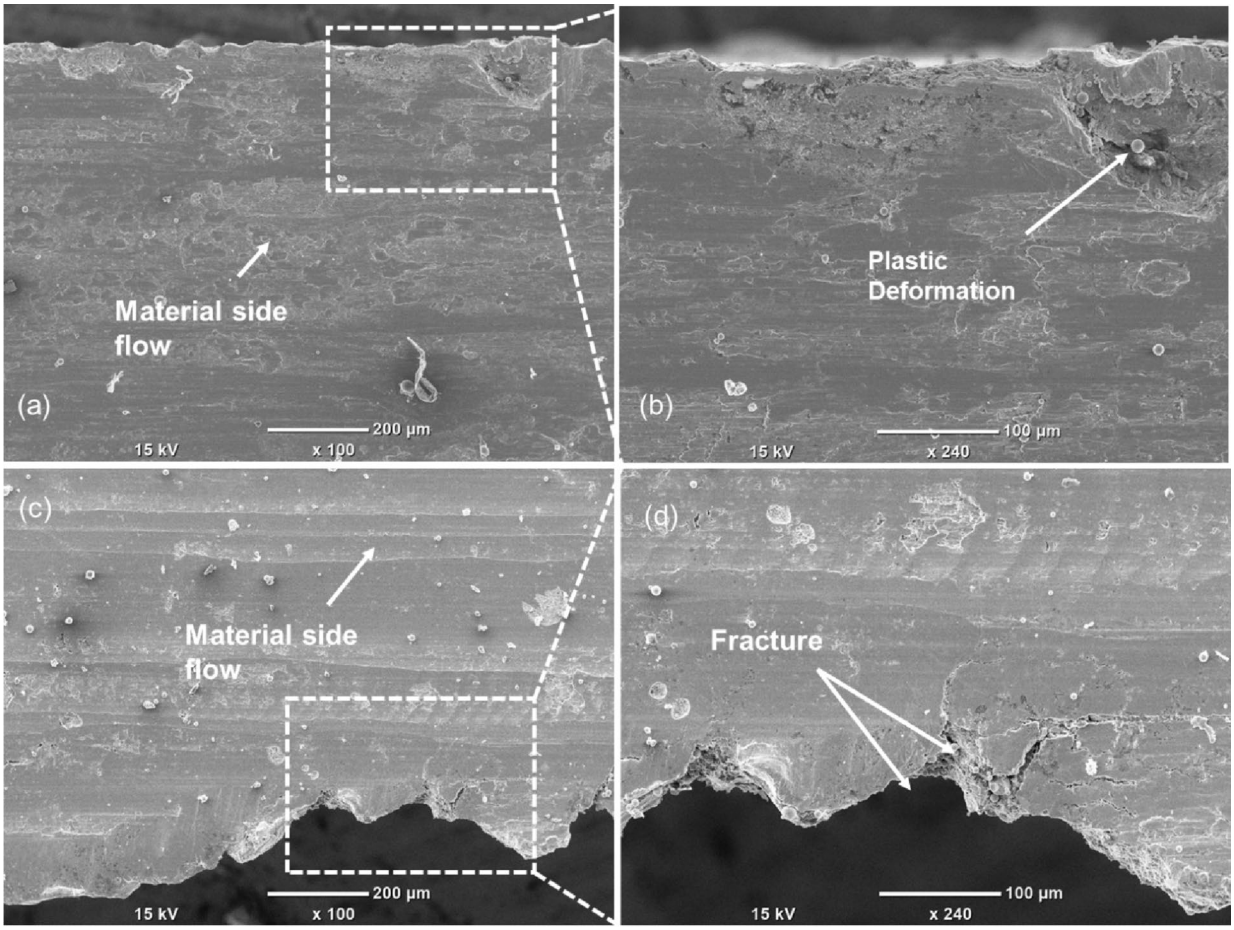

Fig. 16 SEM-based qualitative analysis of hole inlet (**a**, **b**) and exit (**c**, **d**) for Test 7 (DC 53 Steel, 20 m/min, 0.05 mm/rev).

which enables fracture-assisted material separation and segmented chip formation to produce smaller burrs and better edge quality.

Integrated hole integrity index model

Figure 18 displayed the calculated IHII for all the test. The IHII of Test 4 was 0.743 indicated the overall best drilling performance which in turn generated lowest tool wear, better surface finish, reduced diametric error and lower values of burr and machining temperature. Interestingly, this corresponds to D2 material while for DC 53 steel, the IHII was 0.572 which is 23% lower than that of D2 steel. This reduction in IHII was attributed to greater tool wear which in turn translated in greater Ra, higher DE, escalated MT and extended burr height at the hole exit. To further elaborate this, a bar graph is plotted with a decreasing trend of IHII values together with flank wear which shows that relatively higher flank wear values inversely affect the IHII index particularly for Tests 11 and 12 with values less than 0.250. DC 53 steel showed poor IHII values due to greater flank wear and lower hole integrity attributes evaluated herein.

Similarly, the TOPSIS closeness coefficients were determined and plotted using entropy weights derived from the IHII model. Figure 19 presents the calculated TOPSIS rankings in descending order. While the positions for Tests 4, 6, 11, and 12 remain consistent with the IHII findings, the rankings for the remaining tests differ. This variation is expected, as the IHII model relies on a simple weighted summation, whereas TOPSIS calculates closeness to the ideal solution.

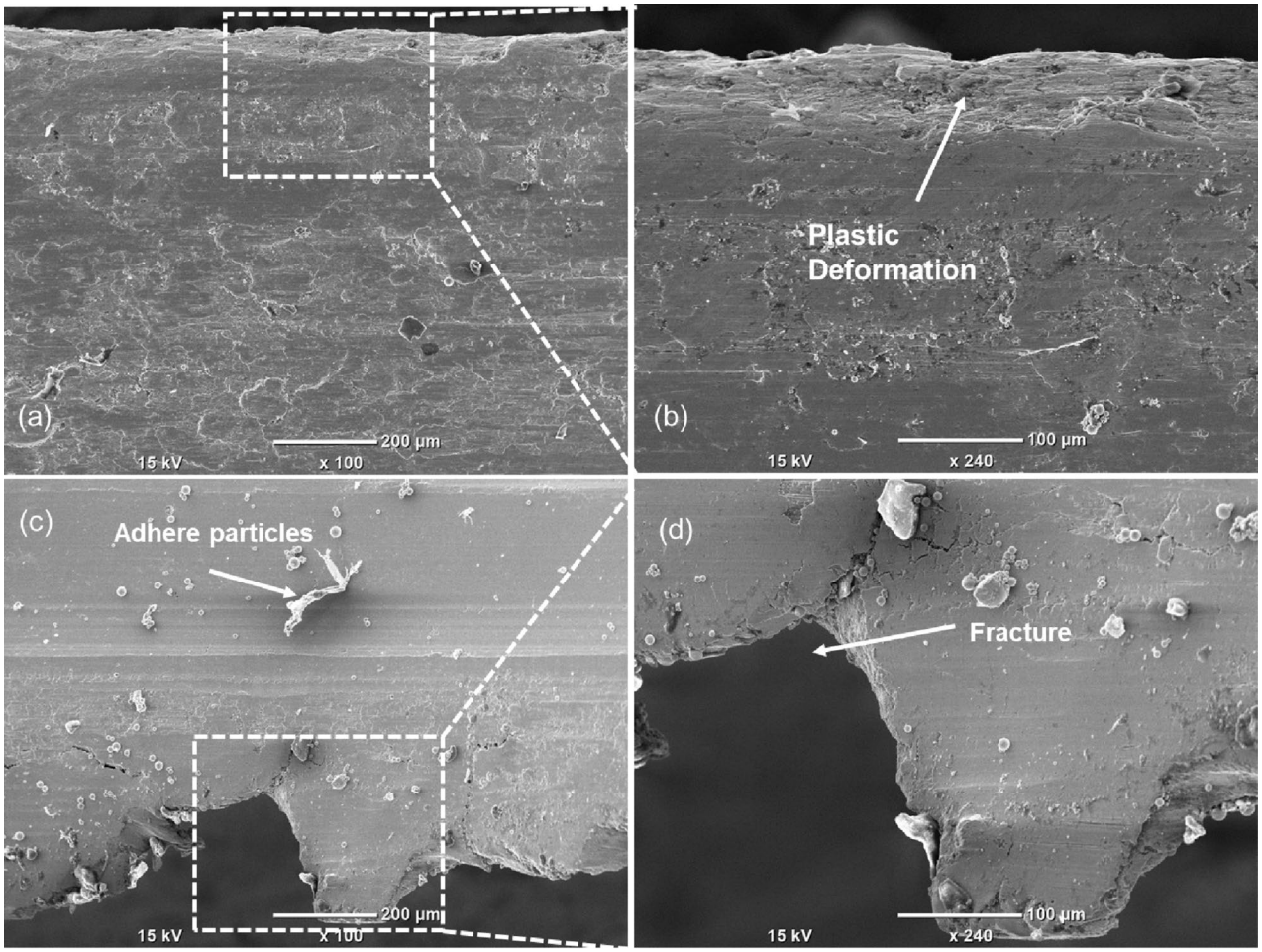

Fig. 17 SEM-based qualitative analysis of hole inlet (**a**, **b**) and exit (**c**, **d**) for Test 9 (DC53 Steel, 20 m/min, 0.10 mm/rev).

Significance analysis

To determine how various machining parameters impacted drilling outcomes, an analysis of variance based on a General Linear Model was conducted. The statistical significance of each parameter was assessed via P-values, and the Percentage Contribution Ratio was employed to measure how much each factor influenced the variance in the responses. Factors with P-values below 0.05 were deemed statistically significant. Table 6 provides a summary of these statistical findings.

As illustrated in Table 6, tool wear was primarily influenced by the workpiece material, which accounted for 40.65% of the total variation ($P=0.003$), with cutting speed also playing a significant role at 33.02% ($P=0.005$). Conversely, the feed rate had a minor, non-significant impact (11.76%, $P=0.126$) on tool wear. Regarding surface roughness, the feed rate emerged as the primary factor, responsible for 58.52% of the variation and exhibiting statistical significance ($P=0.029$). In contrast, cutting speed and workpiece material exerted negligible, statistically insignificant effects ($P>0.05$), suggesting that feed rate was the principal driver of surface quality within the tested parameters. The investigation into diametric error indicated that none of the parameters examined had a statistically significant impact on dimensional accuracy ($P>0.05$). Material and cutting speed each accounted for 13.51% of the variation, while feed rate contributed 7.57%. This implies that the hole dimensional accuracy remained stable across the range of drilling parameters tested. Regarding maximum drilling temperature, workpiece material was the most significant factor (49.31%, $P=0.001$), followed by the feed rate (37.54%, $P=0.004$).

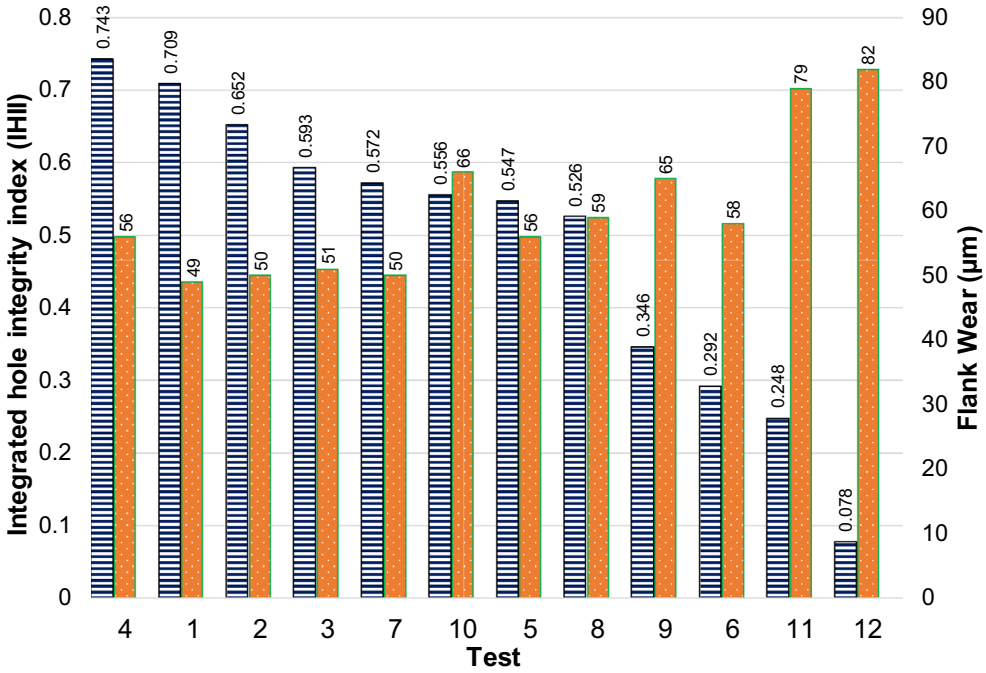

Fig. 18 Integrated hole integrity index (IHII) and flank wear of all tests.

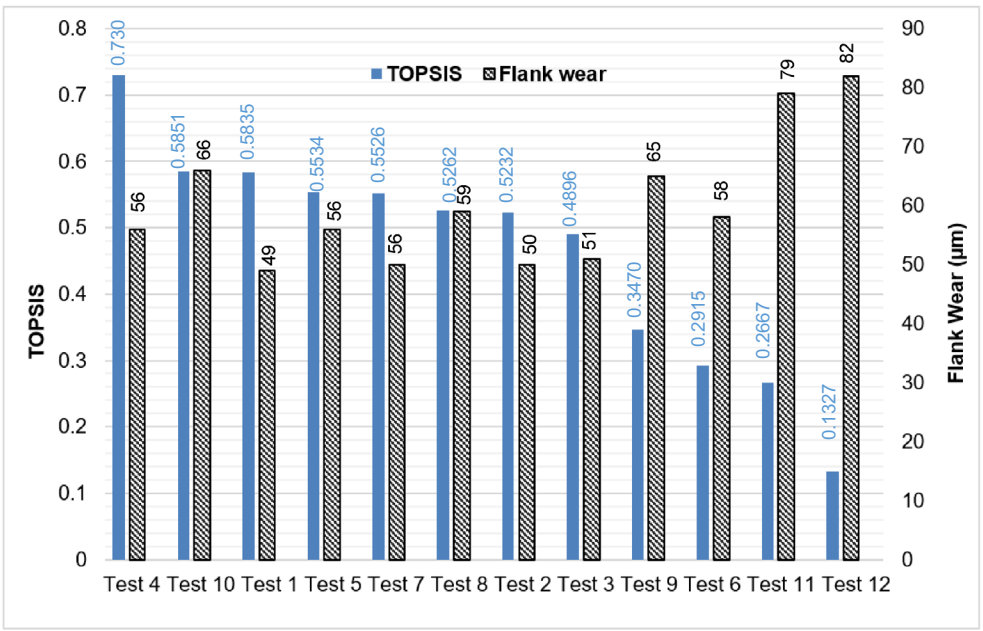

Fig. 19 Bar graph of TOPSIS ranking vs. Flank wear.

Cutting speed had a minimal, non-significant contribution (3.60%, $P=0.148$). Further analysis showed that exit burr height was largely influenced by cutting speed, which drove 79.06% of the total variation ($P<0.001$). While feed rate (12.31%) and workpiece material (8.20%) also had statistically significant impacts, their influence was substantially less than that of cutting speed. Thus, cutting speed is the main factor controlling burr formation during the drilling of D2 and DC53 steels. Overall, the analysis confirms that the primary machining parameter

Table 6 Summary of ANOVA results.

Response	Factor	PCR (%)	*P*-value
Tool Wear	Material	40.65	0.003
	Cutting Speed	33.02	0.005
Surface Roughness	Feed Rate	58.52	0.029
	Cutting Speed	7.75	0.245
Diametric Error	Material	—	>0.05
	Cutting Speed	—	>0.05
Maximum Temperature	Material	49.31	0.001
	Feed Rate	37.54	0.004
Exit Burr Height	Cutting Speed	79.06	<0.001
	Feed Rate	12.31	<0.001

shifts based on the specific response. Workpiece material is the main driver for tool wear and maximum drilling temperature, feed rate most heavily influences surface roughness, and cutting speed is the principal factor for exit burr height. Meanwhile, no single parameter significantly affected diametric error within the tested experimental parameters.

Conclusions

Machining steels such as D2 and DC53 in a dry cutting environment poses significant difficulties owing to their ductility, hardness, poor thermal conductivity, and different microstructures. These properties lead to poor tool life and reduced surface quality of the machined surface. This study explores the different microstructures of both D2 and DC53 steel on drilling when using Indexable drilling inserts and an integrated hole integrity index was determined using the entropy-weighted method.

1. Overall, D2 steel showed lower tool wear as compared to DC53 under the same cutting conditions. The lowest tool wear of 49 µm was observed in Test 1 for D2 steel. The uneven and coarse distribution of carbides in the D2 steel helps create segmented chips, which then reduces friction. However, in DC 53 steel, the fine martensitic structure and even distribution of fine carbides led to longer tool chip contact, producing long chips, which increased wear, particularly at high cutting speeds and feed rates.
2. For both steels, the value of surface roughness increased with an increase in the feed rate and cutting speed. Overall, D2 steel has lower surface roughness values as compared to its counterpart. The lowest surface roughness value of 1.0–4.8 µm was observed in Test 1, whereas for DC53 steel, higher Ra values of 1.9–5.4 µm were observed for the same cutting conditions. The SEM analysis revealed material adhesion and material side flow at higher feed rates. The fine carbide distribution and higher ductility of DC53 steel encouraged the continuous long chips, which resulted in higher Ra values for DC53 steel.
3. During the machining, a higher machining temperature of 353 °C was observed for the DC53 steel. Whereas, for D2 steel, the maximum recorded temperature was limited to 302 °C. For DC53 steel, the ongoing creation of continuous chips makes it harder to get rid of heat, which leads to more heat building up during the drilling process.
4. DC53 exhibited larger deviations due to elevated cutting temperatures, increased elastic recovery, and more significant tool wear. In contrast, D2 steel demonstrated better dimensional stability owing to fracture-assisted material removal and segmented chip formation. All drilled holes displayed positive dimensional deviations in the range of 60–170 µm.
5. In the drilling process, the exit burr height increased with cutting speed, feed rate, and number of drilled holes. The smallest burr height of 175 µm was recorded for D2 steel at 20 m/min and 0.05 mm/rev, whereas DC53 had a maximum burr height of 570 µm at 30 m/min and 0.10 mm/rev. Thus, a deburring operation is recommended for all the holes machined using this method.

6. For holistic drilling assessment, an integrated hole integrity index was calculated. The calculated IHII of Test 4 was 0.743, indicating the overall best drilling performance, which in turn generated the lowest tool wear, better surface finish, reduced diametric error, and lower values of burr and machining temperature. Interestingly, this corresponds to D2 material, while for DC 53 steel, the IHII was 0.572 which is 23% lower than that of D2 steel.

The combination of LM-geometry wiper inserts with central stepped inserts showed good results when dry drilling both types of tool steel.

Limitations, recommendations and future work

Although the present study successfully evaluated the effects of cutting speed within the selected practical machining range, future work may extend the investigation by including additional cutting speed levels. A broader experimental range would allow a more detailed analysis of the relationship between cutting speed and machining performance and further strengthen the generalizability of the findings. One limitation of the present study is that the cutting-edge radius of the indexable inserts was not experimentally measured; therefore, the influence of the minimum uncut chip thickness (size effect) was not assessed. While the relatively high feed rates employed are expected to minimize size-effect influences, future research should investigate the role of cutting-edge geometry and minimum uncut chip thickness on drilling performance and surface integrity, especially under lower feed conditions. Furthermore, the cutting temperature reported in this study was obtained using an infrared thermal imaging system that measures the temperature of the visible workpiece/tool surface rather than the actual temperature at the tool–workpiece interface inside the drilled hole. Owing to the limited line of sight during drilling, direct measurement of the cutting zone temperature was not possible. Therefore, the recorded temperatures should be interpreted as representative surface temperatures that reflect the thermal behavior of the drilling process rather than the exact interface temperature.

Acknowledgements The authors are thankful for the support from the Ongoing Research Funding Program, (ORF-2026-1072), King Saud University, Riyadh, Saudi Arabia.

Author contributions Muhammad Farzik Ijaz: Methodology, Investigation, Funding acquisition and Writing the original draft, Muhammad Zubair Afzal: Conceptualization, Data curation, Writing reviewing and Editing, Sarmad Ali Khan: Conceptualization, Supervision, Writing reviewing and Editing, Samina Ishtiaq: Formal Analysis and Writing reviewing and Editing, Muhammad Umar Farooq: Software, Analysis and Writing reviewing and Editing, Saqib Anwar: Investigation, Validation, Writing reviewing and Editing.

Funding This work is supported by the Ongoing Research Funding Program, (ORF-2026-1072), King Saud University, Riyadh, Saudi Arabia.

Data availability Available upon reasonable request.

Declarations

Competing interests The authors declare that they have no known competing financial interests or personal relationships that could have appeared to influence the work reported in this paper.

Open Access This article is licensed under a Creative Commons Attribution-NonCommercial-NoDerivatives 4.0 International License, which permits any non-commercial use, sharing, distribution and reproduction in any medium or format, as long as you give appropriate credit to the original author(s) and the source, provide a link to the Creative Commons licence, and indicate if you modified the licensed material. You do not have permission under this licence to share adapted material derived from this article or parts of it. The images or other third party material in this article are included in the article's Creative Commons licence, unless indicated otherwise in a credit line to the material. If material is not included in the article's

Creative Commons licence and your intended use is not permitted by statutory regulation or exceeds the permitted use, you will need to obtain permission directly from the copyright holder. To view a copy of this licence, visit http://creativecommons.org/licenses/by-nc-nd/4.0/.

References

1. Liao, Z. et al. Review of current best machining practices in machinability evaluation and understanding for improving machining performance. *CIRP J. Manufact. Sci. Technol.* **50**, 151–184. https://doi.org/10.1016/j.cirpj.2024.02.008 (2024).
2. Alok, A., Kumar, S., Pandey, S. M. & Kumar, A. Review on the effect of surface textured tools in the field of machining. *Adv. Mater. Process. Technol.* **10** (2), 814–832. https://doi.org/10.1080/2374068X.2023.2184580 (2023).
3. Abbas, A. T. M. Comparative assessment of wiper and conventional carbide inserts on surface roughness in the turning of high strength steel. *J. Mater. Sci. Res.* **5** (1), 32. https://doi.org/10.5539/jmsr.v5n1p32 (2015).
4. Machado, A. R. et al. Comprehensive review of advanced methods for improving the parameters of machining steels. *J. Manuf. Process.* **125**, 111–142. https://doi.org/10.1016/j.jmapro.2024.07.044 (2024).
5. Hassan, S. et al. Investigation on tool wear mechanisms and machining tribology of hardened DC53 steel through modified CBN tooling geometry in hard turning. *Int. J. Adv. Manuf. Technol.* **127** (1–2), 547–564. https://doi.org/10.1007/s00170-023-11528-5 (2023).
6. Kang, J. et al. Hot-worked microstructure and hot workability of cold-work tool steels. *Mater. Charact.* **135**, 8–17. https://doi.org/10.1016/j.matchar.2017.11.001 (2017).
7. Rahim, M. S. B. A., Minhat, M. B., Hussein, N. I. S. B. & Salleh, M. S. B. A comprehensive review on cold work of AISI D2 tool steel. *Metall. Res. Technol.* **115** (1), 104. https://doi.org/10.1051/metal/2017048 (2017).
8. Çardaklı, İ. S. & Kalkanlı, A. Effect of solidifcation rate on microstructure and primary carbides of AISI DC 53 cold work tool steel. *China Foundry*. **16** (3), 211–216. https://doi.org/10.1007/s41230-019-8134-6 (2019).
9. Hassan, S., Khan, S. A., Naveed, R., Anwar, S. & Farooq, M. U. Finish dry turning of DC53 tool steel via modified carbide inserts: a study of machining dynamics. *Int. J. Adv. Manuf. Technol.* **132** (9–10), 4505–4523. https://doi.org/10.1007/s00170-024-13594-9 (2024).
10. Binali, R. et al. Advance monitoring of hole machining operations via intelligent measurement systems: A critical review and future trends. *Measurement* **201**, 111757. https://doi.org/10.1016/j.measurement.2022.111757 (2022).
11. Pawanr, S. & Gupta, K. Dry Machining Techniques for Sustainability in Metal Cutting. *Rev. Processes*. **12** (2), 417. https://doi.org/10.3390/pr12020417 (2024).
12. Ajay Kumar, G. V., Ramaa, A. & Shilpa, M. Comparative study of dry machining performance using hybrid textured cutting insert. *Mater. Manuf. Processes*. **39** (12), 1775–1783. https://doi.org/10.1080/10426914.2024.2362650 (2024).
13. Singh, T., Singh, C. D. & Singh, R. A review on minimum quantity lubrication (MQL) assisted machining processes using mono and hybrid nanofluids. *Industrial Lubrication Tribology*. **75** (9), 1054–1076. https://doi.org/10.1108/ilt-05-2023-0131 (2023).
14. Banerjee, A. & Maity, K. Analytical insights into SQL-assisted machining of Nitronic-50 using MT-CVD and MT-PVD inserts. *J. Manuf. Process.* **168**, 350–377. https://doi.org/10.1016/j.jmapro.2026.04.016 (2026).
15. Banerjee, A. & Maity, K. Tribo-mechanical analysis of SQL-assisted turning of nitronic-50 using uncoated WC-Co inserts. *J. Manuf. Process.* **166**, 330–351. https://doi.org/10.1016/j.jmapro.2026.03.041 (2026a).
16. Makhesana, M. A., Patel, K., Ghetiya, N., Binali, R. & Kuntoğlu, M. Evaluation of drilling and hole quality characteristics in green machining aluminium alloys: A new approach towards green machining. *J. Manuf. Process.* **129**, 176–186. https://doi.org/10.1016/j.jmapro.2024.08.059 (2024).
17. Kuntoğlu, M. et al. Sustainable Lubrication Strategies in Eco-friendly Machining of AISI 4140 Steel: Performance and Environmental Impact Analysis using Machine Learning. *J. Mater. Eng. Perform.* **35** (5), 4962–4978. https://doi.org/10.1007/s11665-025-11948-2 (2025).
18. Katam, A. K., Mohanty, R. C. & Kolakoti, A. The role of bio-based cutting fluids for sustainable manufacturing and machining processes: A holistic review. *Mech. Eng. Soc. Ind.* **3** (3), 166–180. https://doi.org/10.31603/mesi.10680 (2023).
19. Pawanr, S. & Gupta, K. Dry Machining Techniques for Sustainability in Metal Cutting. *Rev. Processes*. **12** (2), 417. https://doi.org/10.3390/pr12020417 (2024).
20. Fathallah, B. B., Fredj, N. B., Sidhom, H., Braham, C. & Ichida, Y. Effects of abrasive type cooling mode and peripheral grinding wheel speed on the AISI D2 steel ground surface integrity. *Int. J. Mach. Tools Manuf.* **49** (3–4), 261–272. https://doi.org/10.1016/j.ijmachtools.2008.10.005 (2008).
21. Patil, A. S., Sunnapwar, V. K. & Bhole, K. S. Effect of hybrid tri-nano flood cooling environment and shearing parameters on surface quality with tool health in helical milling of Ti6Al4V. *Int. J. Interact. Des. Manuf. (IJIDeM)*. **18** (10), 7039–7057. https://doi.org/10.1007/s12008-023-01286-9 (2023).

22. Patil, A. S., Sunnapwar, V. & Bhole, K. S. Cumulative effect of Shearing parameters and Ramp angle on Hole surface quality in Ti6Al4V by Helical milling strategy. *Mater. Today Proc.* **113**, 147–151. https://doi.org/10.1016/j.matpr.2023.08.050 (2023a).
23. Anwar, S., Khan, N. A., Khan, S. A. & Raza, S. F. One-Step High-Speed finish drilling of Inconel 718 Superalloy via novel inserts. *Processes* **11** (3), 752. https://doi.org/10.3390/pr11030752 (2023).
24. Ehsan, S. et al. Evaluating tool wear mechanisms, hole integrity and drilling performance of indexable and solid carbide tools on GFRP-Steel stacked composite. *Wear* 576–577. https://doi.org/10.1016/j.wear.2025.206096 (2025).
25. Wang, W., Hua, M. & Wei, X. Friction behavior of SUS 304 metastable austenitic stainless steel sheet against DC 53 die under the condition of friction coupling plastic deformation. *Wear* **271** (7–8), 1166–1173. https://doi.org/10.1016/j.wear.2011.05.023 (2011).
26. Singh, K., Khatirkar, R. K. & Sapate, S. G. Microstructure evolution and abrasive wear behavior of D2 steel. *Wear* 328–329. https://doi.org/10.1016/j.wear.2015.02.019 (2015).
27. Khanna, N. et al. Influence of tool geometry and coating in high speed drilling performance of Additively Manufactured Inconel 718. *J. Tribol.* **148** (7), 072504. https://doi.org/10.1115/1.4071321 (2026).
28. Zielmann, R. P. et al. Effect of cutting fluid reduction on the dimensional quality of holes. *Proc. Institition Mech. Eng. Part. B J. Eng. Manuf.* **229** (8), 331–350. https://doi.org/10.1177/0954405414535769 (2015).
29. Dang, J. et al. Experimental investigation on machinability of DMLS Ti6Al4V under dry drilling process. *Mater. Manuf. Processes*. **34**, 749–758. https://doi.org/10.1080/10426914.2019.1594254 (2019).
30. Shirbavikar, K. et al. Tool Wear Detection Using Image Processing Technique. *Int. J. Innovative Sci. Res. Technol. (IJISRT)*. 2409–2409. https://doi.org/10.38124/ijisrt/25nov1341 (2025).
31. Aboloje, A. E., Sada, S. O., Ekpu, M. & Eyenubo, O. J. Evaluation of the optimal cutting performance of high-speed steel and tungsten carbide cutting tools in the machining of AISI 304 steel. *Int. J. Adv. Manuf. Technol.* **130**, 3609–3617. https://doi.org/10.1007/s00170-023-12909-6 (2024).
32. Hiremath, A., Malghan, R. L., Bolar, G. & Polishetty, A. Comprehensive machinability assessment of Ti6Al4V alloy during drilling and helical milling using sustainable dry condition. *Int. J. Interact. Des. Manuf. (IJIDeM)*. **19** (3), 1987–2002. https://doi.org/10.1007/s12008-024-01964-2 (2024).
33. Jagadish, J. & Ray, A. Optimization of green electrical discharge machining using an integrated approach. *2014 IEEE Int. Conf. Industrial Eng. Eng. Manage.* **1**, 943–947. https://doi.org/10.1109/ieem.2014.7058777 (2014).
34. Bhat, P., Agrawal, C. & Khanna, N. Development of a sustainability assessment algorithm and its validation using case studies on cryogenic machining. *J. Manuf. Mater. Process.* **4** (2), 42. https://doi.org/10.3390/jmmp4020042 (2020b).
35. Rahim, M. S. B. A., Minhat, M. B., Hussein, N. I. S. B. & Salleh, M. S. B. A comprehensive review on cold work of AISI D2 tool steel. *Metall. Res. Technol.* **115** (1), 104. https://doi.org/10.1051/metal/2017048 (2017b).
36. Patil, A. S., Sunnapwar, V. K., Bhole, K. S. & More, Y. S. Experimental investigation and fuzzy TOPSIS optimisation of Ti6Al4V finish milling. *Adv. Mater. Process. Technol.* **8** (4), 3706–3729. https://doi.org/10.1080/2374068x.2021.1971002 (2021).
37. Patil, A. S. et al. RETRACTED ARTICLE: Effective machining parameter selection through fuzzy AHP-TOPSIS for 3D finish milling of Ti6Al4V. *Int. J. Interact. Des. Manuf. (IJIDeM)*. https://doi.org/10.1007/s12008-022-00993-z (2022).
38. Tamura, S., Sekigawa, K. & Matsumura, T. Monitoring of Tool Wear Distribution With Cutting Force Measurement in Drilling. *ASME Conf.* https://doi.org/10.1115/lemp2020-8574 (2020).
39. Čep, R. et al. Surface Roughness after Machining and Influence of Feed Rate on Process. *Key Eng. Mater.* **581**, 341–347. https://doi.org/10.4028/www.scientific.net/kem.581.341 (2013).
40. Padhan, S. et al. Investigation on Surface Integrity in Hard Turning of AISI 4140 Steel with SPPP-AlTiSiN Coated Carbide Insert under Nano-MQL. *Lubricants* **11** (2), 49. https://doi.org/10.3390/lubricants11020049 (2023).
41. Yaka, H. & EngiN, K. Improvement of hole qualities and optimization of machining parameters through experimental and finite element analysis in drilling of AISI D2 cold work steel. *Iğdır Üniversitesi Fen Bilimleri Enstitüsü Dergisi*. **13** (4), 2973–2985. https://doi.org/10.21597/jist.1310601 (2023).
42. Isbilir, O. & Ghassemieh, E. Delamination and wear in drilling of carbon-fiber reinforced plastic composites using multilayer TiAlN/TiN PVD-coated tungsten carbide tools. *J. Reinf. Plast. Compos.* **31** (10), 717–727. https://doi.org/10.1177/0731684412444653 (2012).
43. Bhatnagar, N. D., Singh, I. & Nayak, D. Damage Investigation in Drilling of Glass Fiber Reinforced Plastic Composite Laminates. *Mater. Manuf. Processes*. **19** (6), 995–1007. https://doi.org/10.1081/amp-200034486 (2004).
44. Wei, Y., Ming, W., Chen, M. & An, Q. Effect of drilling parameters and tool geometry on drilling performance in drilling carbon fiber–reinforced plastic/titanium alloy stacks. *Adv. Mech. Eng.* **8** (9), 168781401667028. https://doi.org/10.1177/1687814016670281 (2016).
45. Yaşar, N. & Günay, M. Experimental investigation on novel drilling strategy of CFRP laminates using variable feed rate. *J. Brazilian Soc. Mech. Sci. Eng.* **41** (3). https://doi.org/10.1007/s40430-019-1658-2 (2019).
46. Svensson, D., Andersson, T. & Andersson Lassila, A. Coupled Eulerian–Lagrangian simulation and experimental investigation of indexable drilling. *Int. J. Adv. Manuf. Technol.* **121** (1–2), 471–486. https://doi.org/10.1007/s00170-022-09275-0 (2022).

47. Davidson, S. R. H. & James, D. F. Drilling in bone: modeling heat generation and temperature distribution. *J. Biomech. Eng.* **125** (3), 305–314. https://doi.org/10.1115/1.1535190 (2003).
48. Sun, F. J., Qu, S. G., Li, F. L., Li, X. Q. & Pan, Y. X. Effects of cutting parameters on dry machining Ti-6Al-4V alloy with ultra-hard tools. *Int. J. Adv. Manuf. Technol.* **79** (1–4), 351–360. https://doi.org/10.1007/s00170-014-6717- (2015).
49. Yingfei, G., De Escalona, P. M. & Galloway, A. Influence of Cutting Parameters and Tool Wear on the Surface Integrity of Cobalt-Based Stellite 6 Alloy When Machined Under a Dry Cutting Environment. *J. Mater. Eng. Perform.* **26** (1), 312–326. https://doi.org/10.1007/s11665-016-2438-0 (2016).
50. Jiang, P., Wang, Y., Jia, F. & Zheng, M. Real-time quality monitoring and predicting model based on error propagation networks for multistage machining processes. *J. Intell. Manuf.* **25** (3), 521–538. https://doi.org/10.1007/s10845-012-0703-0 (2012).
51. Soori, M., Habibi, M. & Arezoo, B. Tool Deflection Error of Three-Axis Computer Numerical Control Milling Machines, Monitoring and Minimizing by a Virtual Machining System. *J. Manuf. Sci. Eng.* **138** (8). https://doi.org/10.1115/1.4032393 (2016).
52. Loose, J. P., Ceglarek, D. & Zhou, S. Kinematic Analysis of Dimensional Variation Propagation for Multistage Machining Processes With General Fixture Layouts. *IEEE Trans. Autom. Sci. Eng.* **4** (2), 141–152. https://doi.org/10.1109/tase.2006.877393 (2007).
53. Costa, E. S., Machado, A. R. & Silva, M. B. D. Burr produced on the drilling process as a function of tool wear and lubricant-coolant conditions. *J. Brazilian Soc. Mech. Sci. Eng.* **31** (1), 57–63. https://doi.org/10.1590/s1678-58782009000100009 (2009).
54. Rivero, A., De López, L. N., Aramendi, G. & Herranz, S. An experimental investigation of the effect of coatings and cutting parameters on the dry drilling performance of aluminium alloys. *Int. J. Adv. Manuf. Technol.* **28** (1–2), 1–11. https://doi.org/10.1007/s00170-004-2349-3 (2005).
55. Aamir, M. et al. Effect of Cutting Parameters and Tool Geometry on the Performance Analysis of One-Shot Drilling Process of AA2024-T3. *Metals* **11** (6), 854. https://doi.org/10.3390/met11060854 (2021).
56. Muhammad, A., Kumar Gupta, M., Mikołajczyk, T., Pimenov, D. Y. & Giasin, K. Effect of Tool Coating and Cutting Parameters on Surface Roughness and Burr Formation during Micromilling of Inconel 718. *Metals* **11** (1), 167. https://doi.org/10.3390/met11010167 (2021).
57. Afzal, M. Z. et al. Exploring novel PVD coated wiper inserts' chip breaker designs and feed rates on tool wear and in-depth hole integrity of Ti-6Al-4V alloy when drilling in a dry environment. *J. Manuf. Process.* **131**, 1667–1685. https://doi.org/10.1016/j.jmapro.2024.09.097 (2024k).

Publisher's note Springer Nature remains neutral with regard to jurisdictional claims in published maps and institutional affiliations.

Authors and Affiliations

Muhammad Farzik Ijaz[1] · Muhammad Zubair Afzal[2] · Samina Ishtiaq[3] · Sarmad Ali Khan[2] · Muhammad Umar Farooq[4] · Saqib Anwar[5]

✉ Muhammad Farzik Ijaz
mijaz@ksu.edu.sa

✉ Sarmad Ali Khan
drsarmad@uet.edu.pk

✉ Muhammad Umar Farooq
Umarmuf0@gmail.com

[1] Mechanical Engineering Department, College of Engineering, King Saud University, Riyadh 12372, Saudi Arabia

[2] Department of Industrial and Manufacturing Engineering, University of Engineering and Technology, Lahore 54890, Pakistan

[3] Department of Mechanical, Mechatronics and Manufacturing Engineering (New Campus), Faculty of Mechanical Engineering, University of Engineering & Technology (UET), Lahore, Pakistan

[4] Department of Mechanical Engineering, University of Michigan, Ann Arbor 48109, MI, US

[5] Industrial Engineering Department, College of Engineering, King Saud University, Riyadh 11421, Saudi Arabia